Master of Engineering in Instrumentation and Applied Physics
Physics 524 Fall 2023 professional master's program:
Survey of Instrumentation & Laboratory Techniques

https://physics.illinois.edu/academics/masters
https://courses.physics.illinois.edu/phys524/fa2023/
https://courses.physics.illinois.edu/phys524/fa2023/topics.html

Unit 5: Cooling and thermal management (2 weeks).

Lectures Tuesday and Thursday afternoons 13:00-13:50

Greg Hallewell
Centre de Physique des Particules de Marseille CNRS-IN2P3

Aix-Marseille University
163 Avenue de Luminy
F-13288 Marseille France
http://marwww.in2p3.fr, gregh@cppm.in2p3.fr ; hallewel@cern.ch ; gh23@illinois.edu

October 25, 2023

Some unit preamble…

Cooling and thermodynamics are vast subjects, so this course is about cherry-picking morsels that can be applied to cooling as encountered in everyday situations. This course is intended to be pedagogic and illustrative, with as little theory as possible: - the minimum necessary to explain common phenomena and enable simple performance calculations to be made. Indeed, it is better to introduce the basic concepts and problems, along with illustrations of the practical approaches to solving them.

Some of the examples will draw from the author's experience in cooling systems operating with the silicon pixel tracking detectors of the ATLAS experiment, and other experiments at the CERN Large Hadron Collider. These tracker cooling systems have some commonality with the cooling systems used with silicon processor cores (although with lower power density and lower operating temperatures).

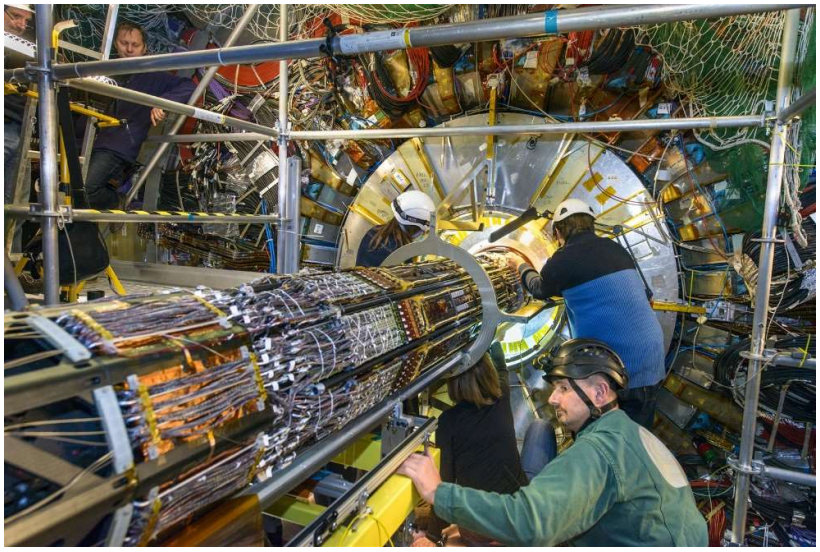

Installation of the ATLAS Pixel detector at LHC: associated cooling tubes visible (CERN)

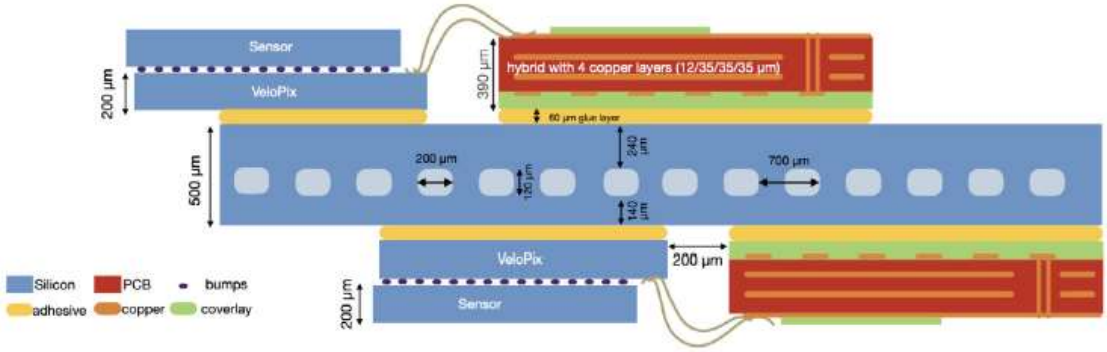

*Micro-channel cooling for the silicon pixel detectors of the **LHCb VE**rtex **LO**cator tracking detector at the CERN LHC – an example of getting the coolant as close as possible to heat-dissipating electronics* **[P1]**

The main focus of this course will however be cooling applications in the temperature range 20C ➔ -20C; the range most commonly encountered in the cooling of computers, processors (and food and drink of course). The course does not address very low temperature cryogenics

at all. Information on the different types of temperature sensors is given in the thermometry section of ˚: *Microcontroller-interfaced sensors* by Michael Davidsaver.

Unit Organization

There will be 4 zoom lectures, each of 50 minutes duration covering the thematic of cooling and thermal management. Parts of these lectures (which are available as Microsoft PowerPoint files) will be devoted to the principles and part given over to related practical experiments in the lab. Students should analyse the data taken in the short experimental sessions for the 1 hour per week tutorial / feedback session, at a time to be decided.

Notes on the unit material "coding" system (see list of course contents)

You will find certain subject material loosely coded "P" or "I":

- Material coded "P" has a corresponding short-duration practical laboratory experiment linked to it;
- Material coded "I" refers to examples that the student should know about as industrial examples of the application of heat removal technology.

References and videos

A set of references, identified in square brackets **[x.x]** is given for each section. A few of these (together with inks in the slides for the 4 lectures) are links to material and videos openly accessible via internet. The emphasis is on practical rather than theoretical reference material. The reference list is far from exhaustive: more references are being added on the internet daily and you will be able to find many more yourselves, and possibly better ones also.

Units

All problems and lab exercises use S.I. units. In some places in the text equivalences in Imperial units are given, but these units are not used for calculations.

Course contents

(1) Thermal Regulation (Code I)

This section introduces devices commonly used to regulate temperature. This section does not go into much detail about the devices or algorithms and does not discuss temperature sensors themselves (thermistors, platinum resistance thermometers, semiconductor devices etc.), which are covered in the thermometry section of *unit 3: Microcontroller-interfaced sensors* by Michael Davidsaver.

(1.1) The humble room thermostat

Fig 1.1 illustrates a simple room thermostat that controls heating or air conditioning. It the simplest form the device has a coiled bi-metallic strip or spring-loaded metallic capsule, which changes shape with temperature, activating a 3-way switch. With the contacts of the 3-way switch closed in one direction (the "too hot" orientation) the thermostat can turn on an air conditioner: in the "too cold" direction it can turn on a heater. Non-electronic thermostats have been use for decades. Despite this apparent obsolescence this device is of interest due to the large thermal inertia of the *room system:* air itself is a fairly poor conductor of heat, so it takes a while for the thermostat to detect that the room has changed enough in temperature for it to change its state back. This leads to a large hysteresis or "*deadband*": the thermostat may only be "accurate" in keeping the room to the desired temperature ± a few degrees, but this stops it from frequently starting or stopping the air conditioner or heater. The feedback in this system is through the air itself.

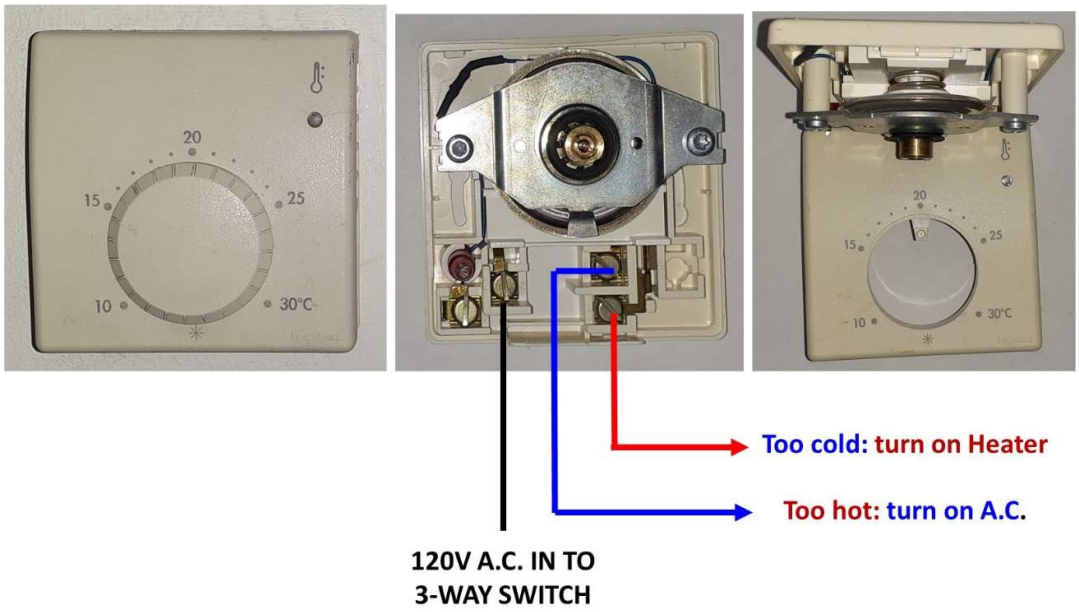

Fig 1.1: *A mechanical room thermostat with a 3-way switch driven by the motion of a temperature-sensitive bi-metallic strip.*

The room thermostat may be electronic using a temperature sensor such as an RTD (PT100) or a NTC thermistor. If the sensor is far from the device doing the heating or cooling air is still

the feedback medium: however the deadband of an electronic controller can be set to be much more fine than the crude action of a purely mechanical thermostat.

When a temperature sensor is fitted close to or even on a structure that is heated or cooled directly, artificially-generated deadband may need to be applied to stop large temperature undershoots or overshoots. This is usually achieved using electronic controllers running a PID (*proportional, integral and derivative*) algorithm implemented in firmware. Figure 1.2 illustrates an example of a low cost ($20 range) device which uses an NTC (negative temperature coefficient) thermistor with a resistance of 10 kOhm at 25 ˚C as a sensor). The outputs of such inexpensive controllers are usually not analog, but switched 120V *with pulse width modulation* in which the duration of the ON signal depends on how close (or not) the temperature is to the set point and how fast it is changing. This kind of switching is also termed "all or nothing" output.

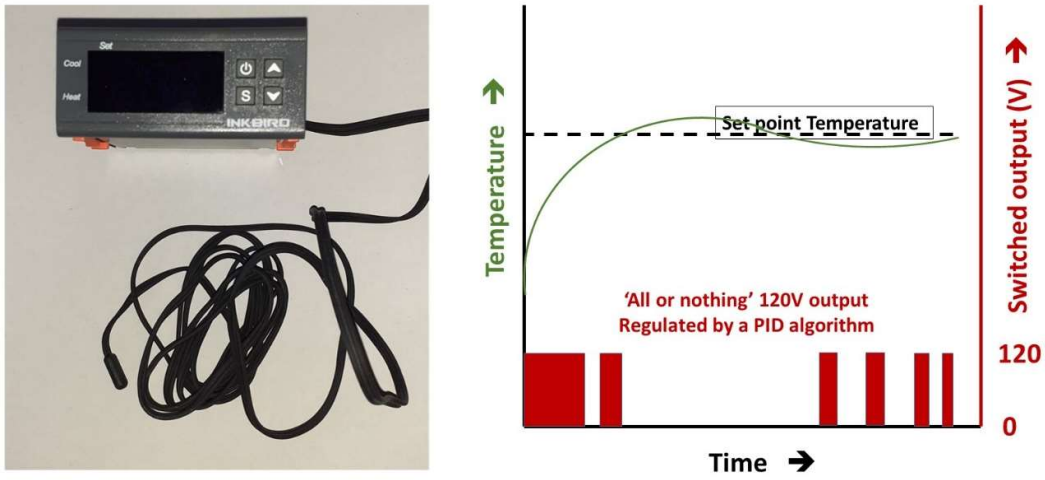

Fig 1.2: *Example of an inexpensive temperature controller with a switched 120V output regulated by a PID algorithm, giving an "all or nothing" pulse width modulated output. The temperature sensor is a thermistor with a negative coefficient of resistance (NTC) with a resistance of 10 kOhm at 25 ˚C.*

(1.2) (PID) Proportional, Integral & Derviative response to a process variable

Proportional, integral and derivative (PID) control uses three correctional terms (K_p, K_I and K_D : proportional, integral and derivative: as illustrated in eq. (1.1), which - when combined - form the collective (time dependent) response $u_{(t)}$ of the control algorithm to differences $e_{(t)}$ between the measured value of a process variable (***PV***) and the setpoint (***SP***) that is to be maintained or reached. The details of the mathematics are too specialised to enter into very far in this short unit but are based on an equation of the form of eq. (1.1). In this expression K_p is the proportional gain, while the second and third terms in the bracket on the right hand side of the expression respectively contain the integral gain K_i and the differential gain K_d.

K_p, K_I & K_D are all "tunable" parameters, while t is the current time (or timestamp) of the measured process value from which $e_{(t)}$ is calculated. The variable τ is the internal integration time which can take on values from a start time to the most recent timestamp t. (This

integration window may have a finite buffer length so the start time gets reset regularly in a rolling advance).

$$u(t) = K_\mathrm{p} e(t) + K_\mathrm{i} \int_0^t e(\tau)\,\mathrm{d}\tau + K_\mathrm{d} \frac{\mathrm{d}e(t)}{\mathrm{d}t}$$

Eq. (1.1)

The sum of the terms on the right hand side of eq (1.1) constitutes the output $u_{(t)}$ of the algorithm

Note that the PID output ***u(t)*** delivers a certain amount of energy to the system. For example in the controller with similar functionality to that shown in fig 1.2, the duration of the "ON" pulses sent from the equivalent of a 3 way switch (a changeover relay inside the controller) will switch power to the system for shorter periods when the temperature is near the set point (to reduce overshoot) than when it is further away. The duration of these pulses will be dynamically controlled via a type of PID algorithm.

The aim of the PID algorithm is to prevent large deviations in either direction between the measured value and the setpoint, and to converge the measured value of the process variable to be as close as possible to the set point as quickly as possible. This convergence is an example of damping or "negative feedback". In addition to the formalism of eq. 1.1 many tuning protocols been developed to converge as smoothly and rapidly as possible. One of these is the Zeigler-Nichols method. Modern industrial process controllers incorporate a Z-N or similar algorithm and can be put into a "learn mode" where the P, I and D terms are automatically varied to "learn" the response of the process system (often called the "transfer function"). The learning time depends of course on the transfer function of the system, but if - for example - a temperature sensor is fitted close or on to a device whose temperature is to be controlled the reaction can be quite rapid, and the learning time correspondingly short.

A very good introduction to the subject of PID control (including animations for different settings of the ***P, I*** and ***D*** corrective terms K_p, K_I & K_D can be found on Wikipedia [1.1]. Fig. 1.3 illustrates a few example screen grabs from this source.

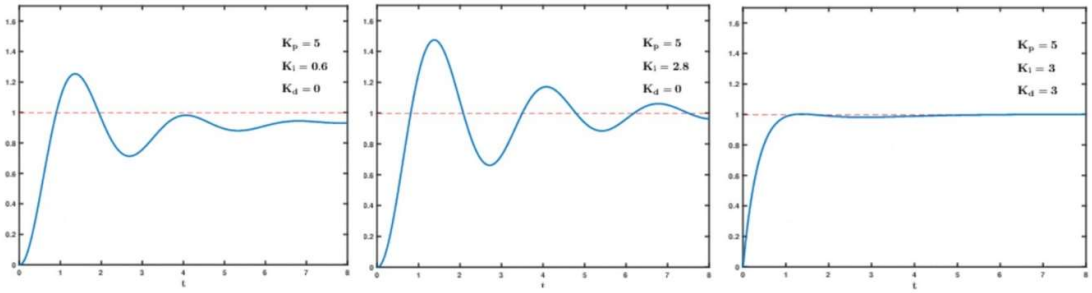

Fig 1.3: *Screenshotted examples (taken from [1.1]) the time-dependent response of the measured value (blue curve) of a process variable (**PV**) following a step change in setpoint (**SP**) when regulated by an automatic learning-mode PID algorithm.*
x-axis*: time (arbitrary units):*
y axis*: measured value of the process value relative to the new set point (taken to be 1).*

It can be seen that the algorithm initially sets a high value of proportional gain to reach and exceed) the new set point, followed by adjustment of the integral gain to bracket the set point, followed by adjustment of the derivative gain to settle at the set point with minimal oscillation amplitude. The oscillation frequency seen early in the convergent cycle depends on the system dynamics: a system with air feedback will be slower than a system with direct contact feedback between a temperature sensor and a heat/cold source.

(1.3) Some other common thermal control devices

The automobile car engine thermostat

The automobile car engine thermostat is a simple thermo-sensitive mechanical valve intended to open more when engine temperature is high, increasing the water-glycol flow through the radiator. The device incorporates a hermetic wax capsule (visible in the left photo of fig 1.4) in contact with the engine coolant. Increasing coolant temperature causes the wax in the cartridge to expand, countering the action of the closure spring (visible in the right photo of fig 1.4) which acts to restrict the flow through the radiator when the engine is cold, so allowing the engine to warm up more quickly.

Fig. 1.4: *An automobile car engine thermostatic valve. Wax in a hermetic capsule (left photo). Expands with increasing coolant temperature, countering the action of the valve closure spring (right photo) which acts to reduce coolant flow through the radiator when the engine is cold.*

The thermostatic heating radiator valve

A thermostatic heating radiator valve works in a similar way to the car engine thermostat shown in fig 1.4. and contains a wax-filled capsule which expands or contracts with the surrounding temperature. The capsule is attached to a pin or valve stem which progressively closes as the temperature of the surrounding area increases, limiting the amount of hot water passing through the radiator. These valves allow individual maximum temperatures to be set for each room in a building. The more expensive valves have setting knobs calibrated in temperature, but most are unsophisticated devices just having knobs with numbered settings from zero (closed) to a maximum (hot-fully open). The hot & cold water mixing valves in bathroom showers work in a similar way.

Fig. 1.5: *Example of heating radiator thermostatic control valve.*

Vapor pressure bulb driven flow valve

These valves are also known as **thermal expansion valves** or **thermostatic expansion valves** (often abbreviated as **TEV**, **TXV**, or **TX valves**) and are often a component in refrigeration and air conditioning systems, used to control the flow of refrigerant released into the heat-removing evaporator (section 3).

A small copper bulb is filled with the same refrigerant fluid as used in the thermodynamic cycle of the refrigeration or air conditioning system, and connected to the vapour capsule of the valve with a copper capillary. The copper bulb is usually strapped to a pipe in the refrigeration system where the temperature is to be sensed. When the temperature at the sensing point is high, implying not enough refrigerant in liquid phase at that point, the pressure of the vapour in the blub rises, pushing on the membrane in the valve and opening the flow orifice in the valve to deliver more refrigerant. The transfer function is rapid as the connections are made onto metal, which is a good heat conductor.

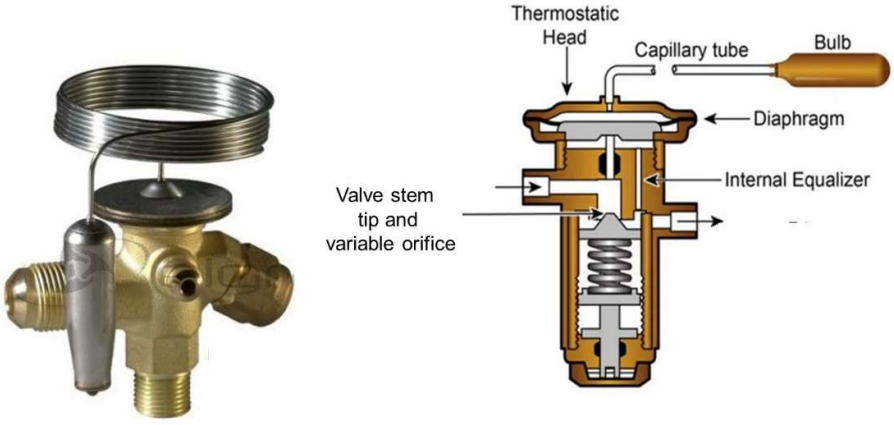

Fig. 1.6*: A thermostatic flow control valve using a vapour pressure bulb as the sensing and regulation element.*

(2) Liquid cooling (Code I, P)

SYSTEMS PACKAGING

Cooling a Superfast Computer

Heat is removed from the CRAY-2 supercomputer by a cooling fluid that flows over each component.

By Richard D. Danielson, 3M Commercial Chemicals Div., St. Paul, Minn., Nick Krajewski and Jerry Brost, Cray Research, Chippewa Falls, Wisc.

A new generation supercomputer, the CRAY-2, uses a novel approach to cooling which will very likely influence computer construction in the future. Made by Cray Research Inc., the supercomputer combines diminutive physical size with very high speed and memory capacity.

The new supercomputer is cooled by immersing the entire computer — power supplies, memory boards, logic circuits and main processors — in an inert, high-dielectric liquid bath. CRAY-2 works sit in a sealed 155-gal tank of 3M's Fluorinert perfluorocarbon, electronic liquid FC-77.

Supercomputer packaging

The CRAY-2 design makes use of significant technological innovations, with capabilities which are an order of magnitude greater than those of its predecessor. These include a clock cycle of 4.1 ns, four background processors for independent or combined tasking, high-speed local random-access memory of 256 million words, and an effective throughput six to 12 times that of the physically larger CRAY-1.

In dramatic counterpoint to its expanded speed and capacity, the CRAY-2 is only about half the size of Cray's earlier system, standing approximately 45-in. high with a diameter of less than 5 ft.

The CRAY-2's relatively small size is a necessity for its blazing speed. Signal propagation times from point-to-point within the system must be extremely short, or the exotic processor and memory circuits cannot do their job. But physical compactness creates enormous heat buildup problems. At very high computer speeds,

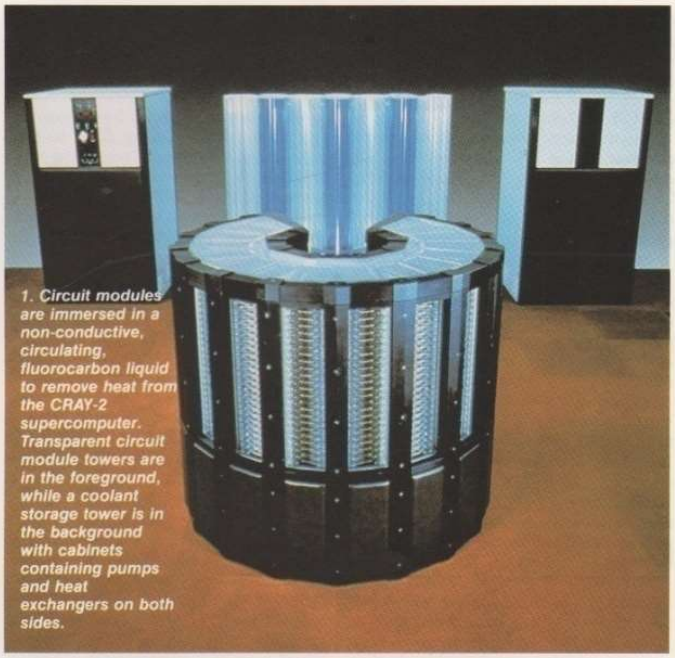

***1. Circuit modules** are immersed in a non-conductive, circulating, fluorocarbon liquid to remove heat from the CRAY-2 supercomputer. Transparent circuit module towers are in the foreground, while a coolant storage tower is in the background with cabinets containing pumps and heat exchangers on both sides.*

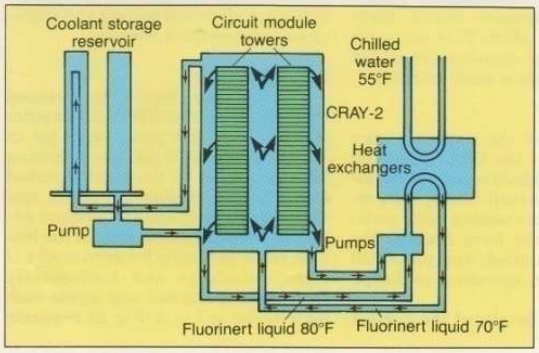

***2. Cooling fluid** is pumped through the circuit module towers and heat exchangers.*

***Fig 2.1: A cold blast from the past**: a computer completely immersed in a liquid coolant [1.2] (which must of course be non-conductive!!): here 3M FC-77® per-fluorocarbon [1.3]. Such fluids have very high Global Warming Potential (GWP_{20y}: 5000-10000* CO_2) and are being progressively replaced with new compounds.*
(Note the liquid pumps and the fluorocarbon / water heat exchanger).

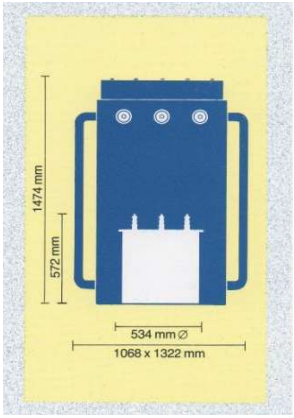

***Fig. 2.2: Other examples**: cooling an airborne military radar transmitter, cooling a transformer (traditionally using sulfur hexafluoride SF_6,: GWP_{20y} of around 23000*CO_2)*

From figure 2.1 we see that the Cray cooling system immerses the computer in the FC-77 primary coolant, which is an electrical insulator. The primary coolant acquires heat from the computer, rising in temperature. This heat must be removed from the primary coolant to prevent it boiling. (In this atmospheric pressure system that would occur for FC-77 at around 206 ˚F, (97 ˚C) [1.3]). Heat is removed from the FC-77 coolant using a cold secondary coolant, in this case "chilled" water at 55˚F (12.8˚C): a commonly-used cooling water temperature in industrial plant. The heat in the FC-77 is *exchanged* to the colder water, heating it up. That water is itself cooled externally and the heat extracted from it: ultimately in exchange with a high flow of air.

In the following subsections we will explore some simple physics on which heat exchangers, and the temperature rise in fluids depend.

(2.1) Heat capacity, temperature rise vs. power and flow rate (Code P)

A heated fluid will rise in temperature according to its mass, ***m*** (kg), the heat energy it has to absorb, ***Q***, (Joules) and its own heat capacity, ***C***. The heat capacity of a fluid (liquid or gas) is expressed in units of $J.kg^{-1}.K^{-1}$) and relates the energy in Joules needed to raise the temperature of 1kg of the fluid by 1 ˚C or 1 Kelvin (K).

Table 2.1: Approximate heat capacity of common fluids and materials (not a phase change situation)

Material	C: J/(kg.°C)	Material	C: J/(kg.°C)
Air (20 ˚C, 1 bar)	1006 [2.1]	Mercury	126
Aluminium	887	3M NOVEC® 649 (liq.) (20 ˚C)	1103 [2.2]
Brass	920	Platinum	150
Copper	385	Silicon	710
3M FC-72® (liq.) (25 ˚C)	1100 [2.3]	Silver	236
Glass	792	316 Stainless Steel	468
Gold	130	Tin	226
Helium (20 ˚C, 1 bar)	5192 [2.1]	Titanium	521
Hydrogen (20 ˚C, 1 bar)	14288 [2.1]	Tungsten	133
Iron	462	Water (liq.)	4187 [2.1]
Lead	130	Zinc	389

We now consider a practical situation: we have a source of heat, ***P***, in Watts (Joules of energy per second: $J.s^{-1}$). We wish to evacuate this heat using a cooling fluid, but what mass flow $\dot{m}$ (kg per second: $kg.s^{-1}$) do we need, and by how much can we allow the temperature in the fluid itself to rise (ΔT, ˚C)? The temperature rise in the liquid is related to the power absorbed by it and its heat capacity via:

$$\Delta T = \frac{P}{C * \dot{m}} \tag{2.1}$$

Problem (2.1) – see also separate sheet:

A core processor chip in a PC dissipates 100W of heat. The user has attached a liquid-channel cooling block directly to it, through which coolant liquid can flow.

The user has a choice between water or a non-conductive modern liquid coolant with GWP=0 (3M NOVEC® 649 [2.2]). What is the mass flow $\dot{m}$ of (1) water and (2) 3M NOVEC® 649 needed to ensure that the coolant liquid temperature rise ΔT is limited to 10 ˚C?

In practice of course, heat must be channelled into the cooling fluid. To do this it must flow through the thickness of the core processor chip silicon package, through the adhesive or thermal grease that bonds it to the cooling block and through the wall of the cooling block into the fluid. All these materials have thermal resistances which add up, resulting in the silicon chip operating at a higher temperature than the cooling fluid circulating through the block. We will revisit this later.

(2.2) Thermal Conductivity, Thermal resistance – getting heat into a coolant

Thermal conductivity and thermal resistance can be considered in a similar way to electrical conductivity and resistance, with expressions similar those derived from Ohm's law.

The temperature difference, δT (K) across a thermal interface (which can be a good thermal conductor like a metal or a poor conductor like a thermal foam insulator) of thickness ***l*** (m) when a power density of ***q*** ($W.m^{-2}$) is applied to one side is given by:

$$\delta T = \frac{q.l}{k} \tag{2.2}$$

where ***k*** is the thermal conductivity of the interface expressed in SI units of $W.m^{-1}.K^{-1}$

Alternatively eq (2.2) can be expressed in terms of the thermal *resistance*, ***R*** (expressed in SI units of $m.K.W^{-1}$) of the interface as follows:

$$\delta T = q.\,R.\,l \tag{2.3}$$

Equation (2.3) has a similar form to that of the expression linking the voltage drop, δV, along a wire of cross sectional area, ***a,*** and length, ***l,*** with its resistivity, ***r***, in Ohm-metres:

$$\delta V = \frac{I.r.l}{a} \tag{2.4}$$

where ***I*** is the current (Amperes). Clearly (***I/a***) in equation (2.4) is the current flux, in $A.m^{-2}$, in direct analogy to ***q*** in equation (2.3).

Table 2.2 shows approximate values of thermal conductibility for some common materials.

Table 2.2: Approximate thermal conductivity of some common materials with references [where given]

Material	Thermal Conductivity $W.m^{-1}.K^{-1}$	Application
Air (20 ˚C, 1 bar)	0.026??? [2.1]	Insulator
Aluminium	236	Good elec & heat conductor
Asbestos (200 ˚C)	0.21	Historic insulator (hazardous)
Beryllia (ceramic)	285 (room temp)	Heat spreader (hazardous)
Brass	109–160	Good elec & heat conductor
Copper	400	Very good elec & heat conductor, cooling systems
Cork	0.043	Insulator
Diamond (CVD wafer)	2300	Heat spreader
Dow Corning 340 heat conducting paste	0.67	Demountable thermal connection heat source ➔ heat sink
3M FC-72® (liq.) (25 ˚C)	0.06 [2.3]	Cooling liquid
Glass	0.935	
Glass Fiber (20 ˚C)	0.042	Insulator
Gold	312	Electrical connections
Graphite	151	Heat spreader
Lead	35	Electrical connections
Mica (50 ˚C)	0.43	Heat resistant Electrical Insulator
3M NOVEC® 649 (liq.) (25 ˚C)	0.06 [2.2]	Cooling liquid
Rockwool (20 ˚C)	0.034	Insulator
Silver	425	Very Good elec & heat conductor
Silicon	148-150	Active semiconductor
304, 316 Stainless Steel	14-18 (room temp)	Poor heat conductor (for a metal), cooling systems
STYCAST® 2850 (Emeron & Cuming)	1.02-1.68 [2.4]	Thermally conductive epoxy: permanent thermal connection heat source ➔ heat sink
Urethane Foam (Rigid) (20 ˚C)	0.026	Insulator
Water (20˚ C)	0.613	Cooling liquid

Problem (2.2) – see also separate sheet:

A core processor chip in a PC dissipates 100W of heat. The chip has a (3 cm x 3cm) square profile. The user has attached a (3 cm x 3cm) square channelled copper block on top of it, through which coolant liquid can flow to cool the processor. The cooling block makes contact with a thin metal jacket on top of the chip through a 100 micron layer of Dow Corning 340 thermally-conducting grease.

The processor chip package itself is 3 mm thick in total (as illustrated in the figure), made from a 1 mm-thick active silicon layer that is centrally-sandwiched with 1 mm of ceramic encapsulant above and below it. The ceramic fill has a thermal conductivity of 200 $Wm^{-1}.K^{-1}$.

Note: the heat is dissipated in the doped semiconductor implanted into the surface of the active silicon layer ***facing down*** towards the connector to the mother board, and must pass through 1 mm of silicon substrate in the opposite (up) direction on its way to the cooling block. Any heat loss by conduction through the connector pins to the mother board can be ignored. The very small thermal resistance of the thin topside metal jacket can also be neglected in the calculation; you can pretend that it isn't there.

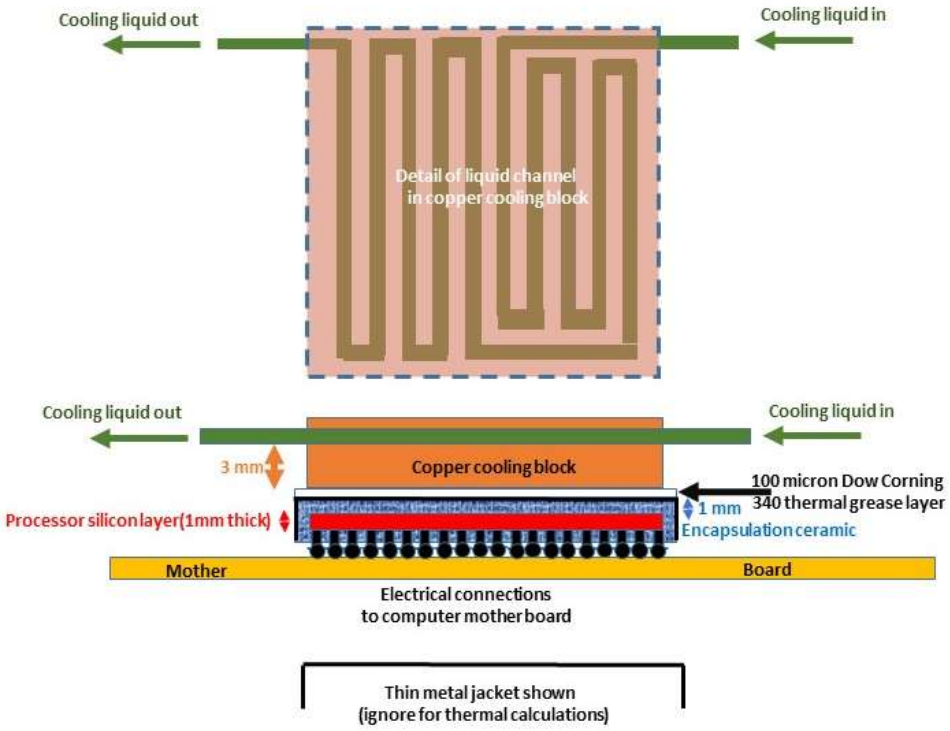

Fig 2.3: *Thermal paths in the cooling of a silicon processor chip (local channel)*

The heat from the chip can be thought of as passing through 1 mm of silicon and a further 1mm of ceramic before passing through a 100 micron (0.1 mm) thick layer of Dow Corning 340 thermal paste, and finally through the copper cooling block with an effective thickness of 3 mm before reaching the cooling liquid channel, as shown in the figure.

Coolant enters the cooling block and follows a tortious path to try to extract heat as uniformly as possible. The high transverse thermal conductivity of the copper block helps

spread the heat transversely over the whole (4 cm x 4 cm) between the wiggles of the coolant channel.

Problem (2.3) questions;

For the first 4 questions you can consider that the coolant to enters the block 20 ˚C and leaves at 30 ˚C. The average temperature of the liquid in the cooling channel can thus be taken to be 25 ˚C.

What are the (progressively-increasing) temperatures on the following surfaces;

- The surface of the copper block in contact with the top face of the Dow Corning 340 thermal grease film (**A**)? (This is 3mm from the plane of the coolant channel)
- The surface of the ceramic in contact with the bottom face of the 100 micron Dow Corning 340 thermal grease film (**B**)?
- The hot (downfacing) side of the1 mm thick processor chip itself (**C**)?
  Note: you have to consider the thermal resistance of two materials in series to get to this figure.
- Which material contributes the biggest temperature difference (temperature difference across itself)?
- What method would you use to reduce the contribution of this layer (mechanical solutions acceptable)?

Building on knowledge

- The user has a choice between water or a non-conductive modern liquid coolant with GWP = 0 (3M NOVEC® 649 [2.2]), but the pump available can only circulate a maximum of 3 grams per second (a mass flow of 0.003 $kg.s^{-1}$) of any liquid. What is the input temperature of NOVEC 649 to the copper cooling block to maintain an average temperature in the block cooling channel of 25 ˚C? (Hint: this calculation uses the concept of coolant heat capacity and mass flow from the previous problem.

(2.3) Fluid-fluid Heat Exchangers

Fig 2.4 *Example of a "perfect" (full contact) heat exchanger in which all 3 phases of matter interact (no intermediate surfaces):*

- *solid fresh water ➔ sea water (water with around 35 kg/tonne of salt, which acts as a freezing point depressant);*
- *solid fresh water ➔ air*
- *peripheral fresh meltwater ➔ sea water and air ;*

(Picture credit: TheRiderPost.com: https://www.theriderpost.com/lifestyle/environnement/iceberg-titanic-sechoue-cote-canada/)

Beautiful but something perhaps you would rather wish you were not witnessing on a Sunday afternoon bike ride along the coast.

We saw in fig 2.1 and 2.3 two different types of heat exchange. In the case of the Cray computer heat from the computer is directly dissipated into the FC77 primary coolant and is transported to an intermediate heat fluid-fluid exchanger where the heat is transferred to circulating chilled water. Though not shown in Fig 2.1 the heated water in turn gives up its heat to air in a cooling tower of which many examples in differing geometries can be seen around power stations and data centers.

In a sense fig 2.3 of problem 2 is also an incomplete story: how does the water (or NOVEC 649 fluid) give up its heat to come back cooler in a closed circuit back to the cooling block?

We will look at some typical heat exchangers in this section. We will see that they fall into several common categories (this is no means an exhaustive list however), some of which we will meet again later. A ***red*** color code is used for a hotter fluid, ***blue*** for cooler fluid

I. ***Hot Liquid to cool liquid :*** liquid in circuit (2) takes heat from liquid in circuit (1); **Examples:** two common examples are the "shell and tube" and "parallel plate" geometries. In the parallel plate geometry, the liquids in the two circuits pass through alternate chambers. Heat is transferred through the walls, which are also imprinted with 3-D features to stir up the liquids to cause turbulence, which improves the heat transfer.

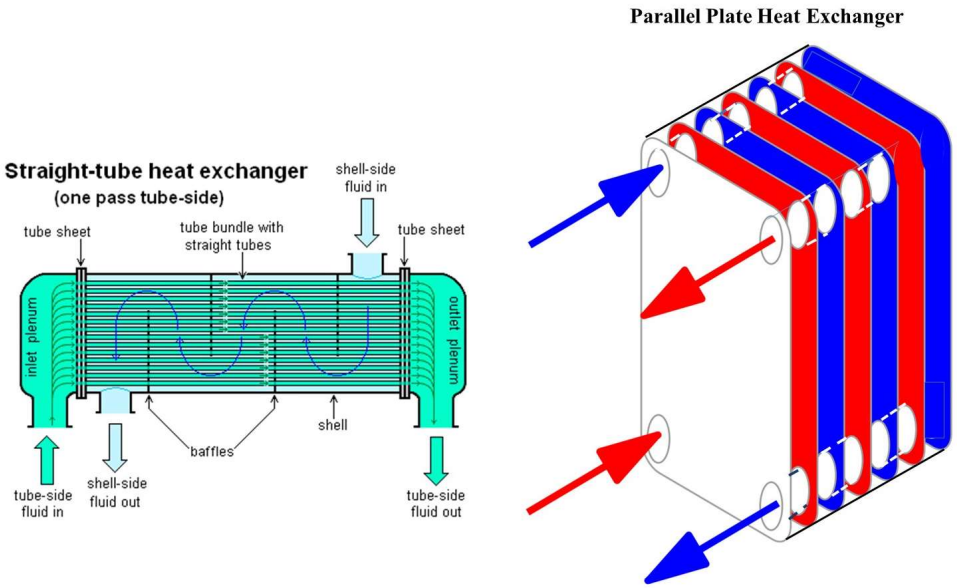

Fig 2.5: *Examples of liquid-liquid heat exchanger geometries (these can also be used in evaporators and condensers)*

II. ***Hot Liquid to cooler gas :*** where a flow of gas in circuit (2) is directed through some kind of finned radiator (possibly fan-assisted). Propelled gas flow in circuit (2) takes heat from hot Liquid in circuit (1). **Example:** an automobile radiator and fan, cooling water from an internal combustion engine;

Fig 2.6: *Example of a liquid ➔ gas heat exchanger geometry - automobile radiator*

III. ***Gas (air) to (liquid ➔ vapor) : an evaporator:*** the heat is taken a from gas in a closed volume (which can be considered as "circuit' (1) which is in contact with the tubes and fins of a heat exchanger cooled by a liquid flowing in circuit (2). In doing so the liquid in circuit (2) changes phase to a vapour. We shall see that a much lower mass flow of coolant is needed than in the case of a liquid in circuit (2) that did not change phase when evacuating heat. **Examples:** the extraction of heat from air inside a domestic refrigerator: the extraction of heat from air that is to be fan-blown into a closed volume: an air conditioner for a house or an automobile.

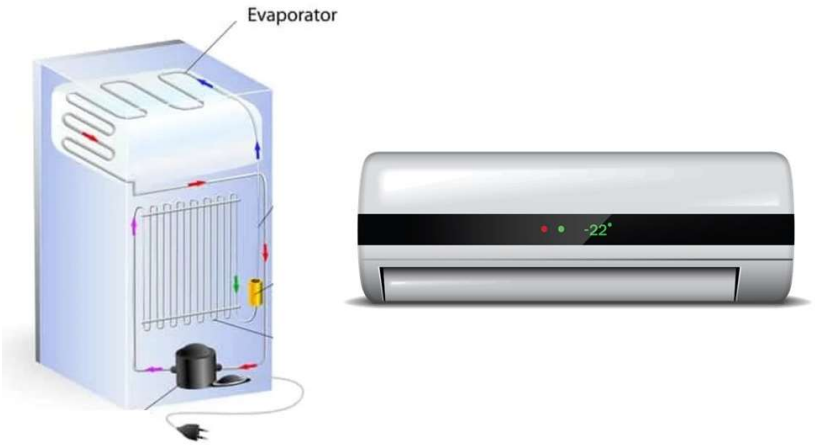

Fig 2.7: *Everyday examples of common forms of evaporative heat exchanger.*

IV. ***Hot (Vapor ➔ liquid) to cooler gas: a condenser:*** the heat is given up from a hot vapor to a cooler gas volume in contact with the tubes and fins of a heat exchanger. In doing so the vapor in circuit (1) condenses to a liquid.

Examples:

- the dumping of heat extracted by evaporation of a coolant from the inside of the closed volume of a domestic refrigerator into the air of the kitchen, which can be thought of as "circuit" (2)
- the dumping of heat extracted by evaporation of a coolant from the inside a house into the outside air, which can be thought of as "circuit" (2).

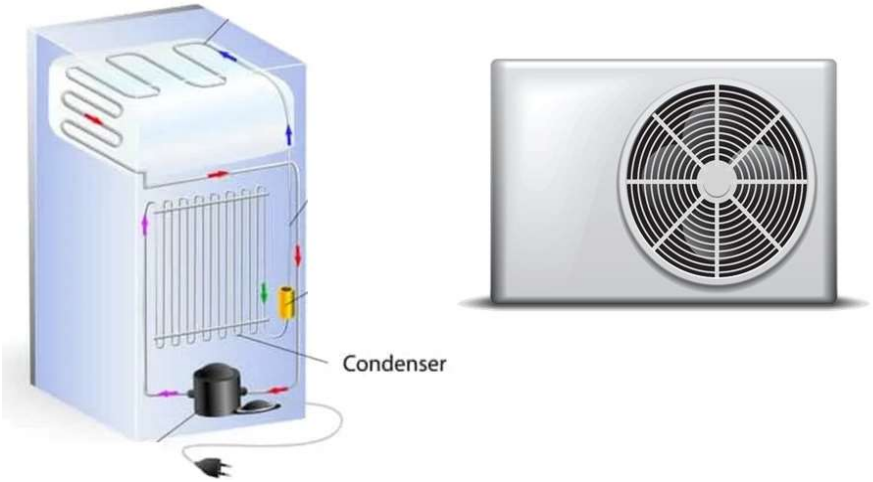

Fig 2.8: *Everyday examples of common forms of condensing heat exchangers.*

V. ***A variant of III: Hot Gas (A) to (pressurised liquid ➔ superheated vapor (B)) : an evaporator:*** the heat is taken a from hot air (circuit (1)) passing through tubes in a volume of liquid (circuit (1)), which becomes a high pressure vapour capable of doing mechanical work.

Examples: Water boiler in a steam turbine-powered ship or a steam railroad locomotive. In both cases the exchanger performs two steps; (a) evaporating water to make saturated steam or "steam over water" (b) passing that saturated steam again through heated pipes to a reach a higher temperature (called superheating), before passing it to turbines (ship) or cylinders and pistons (steam locomotive).

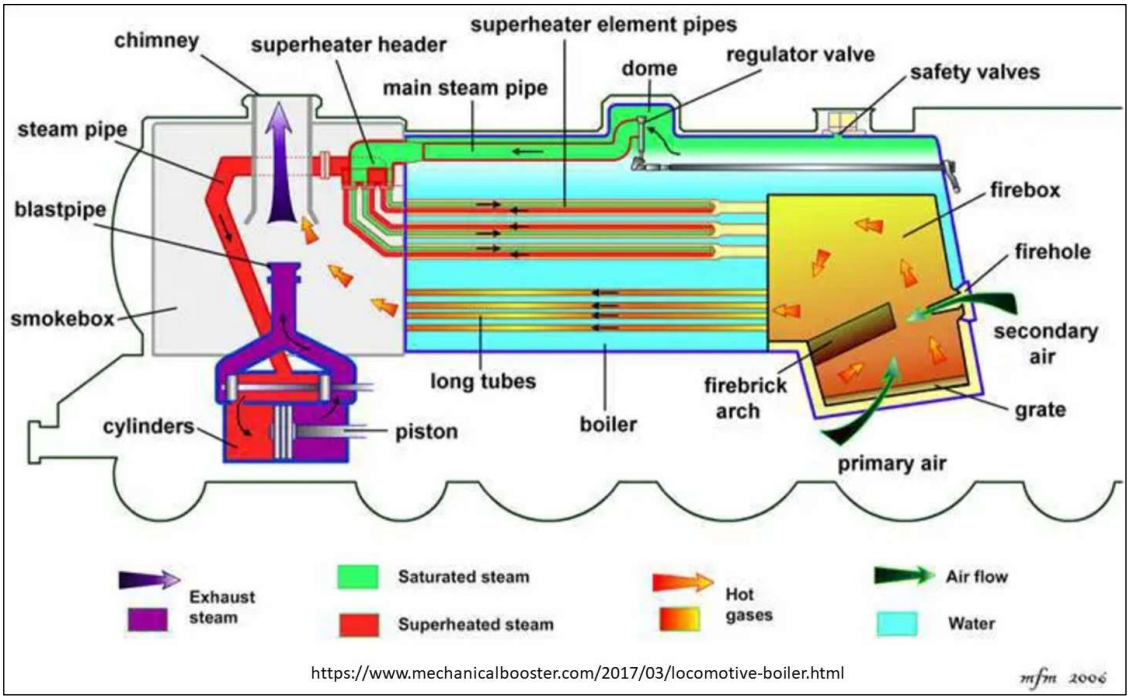

Fig 2.9 *Another form of evaporative heat exchanger: the steam locomotive*

VI. ***A variant of IV: (Hot vapor ➔ liquid) (A) to cool liquid (B): a condenser:*** the heat is given up from a hot vapor in circuit (1) to a liquid in circuit (2) which is in contact with the tubes and fins of a heat exchanger. In doing so the vapor in circuit (1) condenses to a liquid.

Examples: the straight tube heat exchanger shown in (**I**) above is an efficient geometry for this. Cooling liquid can be passed through the tubes linking the two end-domes while the vapour to be condensed back into liquid enters the central space around the tubes, on whose surface it condenses and falls as "rain"**.** The tubes near the bottom of the cylinder help keep the condensed liquid cold. This was carried out on a massive scale in steam turbine powered ships where boiler feedwater in a closed circuit was evaporated in boilers, passed through turbines and then recondensed in counterflow with cold seawater drawn through grilles in the ship's hull.

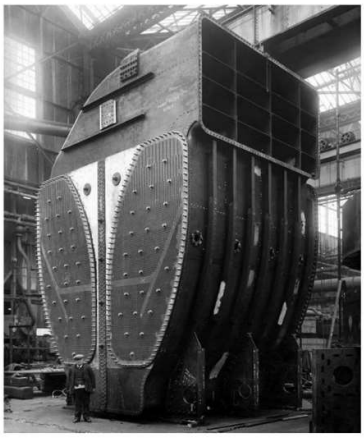

Fig 2.9*:* RMS Queen Mary (now at Long Beach, CA) and a boiler feedwater condenser
Ship completed 1936, John Brown shipyard, Clydebank, Glasgow, Scotland
Displacement: 77,400 long tons (78,642 metric tons)
Length 1,019.4 ft (310.7 m): Beam: 118 ft (36.0 m), Height: 181 ft (55.2 m)
Draught: 38 ft 9 in (11.8 m), Decks: 12
Installed power: 24 × Yarrow boilersPropulsion: 4 × Parsons geared steam turbines,
4 shafts, 200,000 shp (150,000 kW) Speed: 28.5 kts (52.8 km/h; 32.8 mph)

VII ***Hot liquid to cooler gas:***

Example: A water cooling tower of the kind typically used at power stations and big industrial plants. Secondary hot water from a heat exchanger cooling an industrial process is pumped to the top of a cooling tower and sprayed into a counter flow of air. Water is thus cooled and collected in the bottom pond. The circuit is however open, some water escapes as water vapour and must be replenished, while that collected in the bottom pond must be filtered on its way back to the heat exchanger.

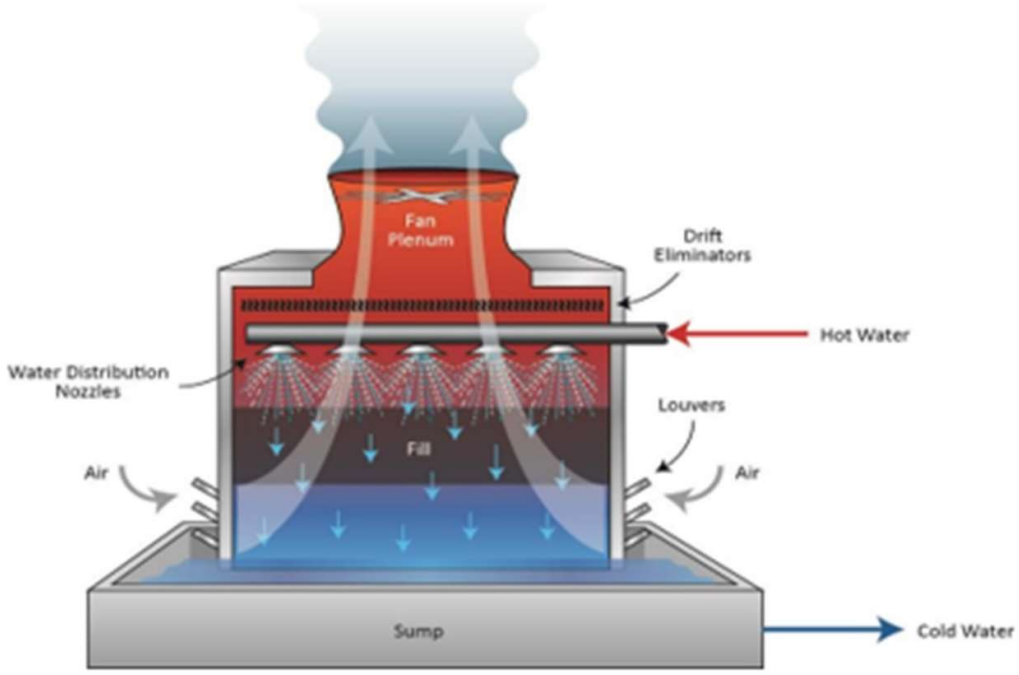

We have seen in the examples of some of the heat exchangers above that a phase change can occur in one of the fluids. Changing the phase of a fluid requires the right combination of temperature and pressure, and requires a lot of energy to achieve. Indeed: phase change is a very good way to achieve cooling with a much smaller flow of coolant than in a monophase system.

We will now go on to explore the energy uptake capabilities of phase change cooling.

(3) Phase change cooling (Code I, P)

In the previous section we saw in the examples of some of the heat exchangers that a phase change can be configured to occur in one of the fluids. Changing the phase of a fluid requires the right combination of temperature and pressure, and represents a big uptake of energy. Indeed: phase change is a very good way to achieve cooling with a much smaller flow of coolant than in a monophase system, as we shall see in these sections.

We will now go on to explore the energy uptake capabilities of phase change cooling.

(3.1) The concept of "latent heat" or enthalpy

Materials can contain a huge amount of energy, and we are not even talking about $E = mc^2$ (nor will we in this course). Imagine the kettle in your kitchen that holds 1 litre of water and has a power rating of 2000 Watts. (You can ignore the loss of heat through the kettle wall to the kitchen for now). You turn the kettle on and note that the kitchen temperature is 20 ˚C. In just under 3 minutes on the kitchen clock (167 seconds later) the water is boiling and bubbling nicely: 1 kg of water has been raised 80 ˚C in temperature for a total delivered electrical energy of 334.7 kilojoules (***it already sounds like a lot: did you need to use this much energy just to boil water for one cup of mint tea?).*** The bell rings: somebody's at the front door and you forget to switch off the kettle, which doesn't have an automatic cut out at 100 ˚C. Some time later you smell a nasty smell coming from the kitchen, which is full of steam. The kettle is empty and finally its thermal interlock trips. You look at the kitchen clock and see that almost 19 more minutes have passed! How much extra energy was wasted boiling away that water into steam at 100 ˚C while you were outside? **Answer**: around 2.25 Mega Joules*! This is around eight times more than you used to raise the liter of water to its boiling temperature for that cup of tea.

*The amount is calculated from the 2250 $kJ.kg^{-1}$ latent heat (or "enthalpy") of evaporation, of water at atmospheric pressure (1 bar) where the evaporation temperature is 100 ˚C.

So what is enthalpy in thermodynamic terms?

Well, the key here is in the "*dynamics*" of the word "thermodynamics". Thermodynamics is the science of the *changes* in key parameters of material systems: pressure, temperature and energy being carried, in response to *perturbations* applied to the system caused by the delivery of external heat energy, the extraction of energy from the system and by the application of mechanical work to the system, or indeed making the system perform mechanical work.

Enthalpy (***H***) is usually expressed in terms of the internal energy (***E***) of a system and its temperature ***T,*** *volume* ***V,*** and pressure ***P***. for example:

$$H = E + P.V \tag{3.1}$$

However the internal energy of a system is hard to measure directly. The energy carrying capability of fluids depends on factors including their chemical composition and density. As we have seen in table 2.1: perhaps surprisingly, liquid water (molecular weight 18) has a much higher heat capacity at constant pressure (***Cp*** = 4181 $J.kg^{-1}.K^{-1}$ at 25 ˚C) than fluids with much higher molecular weights, including modern refrigerants. Its eenthalpy of evaporation is also much higher.

The *absolute* enthalpy, ***H***, of a system can perhaps be thought of as a quantity of energy that contains a baseline energy on top of which *energetic changes* (*thermodynamic changes*) of interest occur. In terms of a particular material it can be expressed in $kJ.kg^{-1}$.

(3.2) Example of a closed-loop thermodynamic refrigeration cycle

Figure 3.1 illustrates a ***pressure-enthalpy (p-H) diagram,*** taking as an example **a** domestic refrigerator operating in a closed-loop thermodynamic cycle with R404A[1]* refrigerant and showing ***isotherms***: lines of constant temperature. The diagram may look daunting but once you get to know your way around the loop it's not so intimidating. The p-h diagram is divided into three zones with a division occurring at the critical temperature and pressure T_{Crit}, P_{Crit} which at the apex of the central "dome" region:

- to the left of T_{Crit}, but at pressures no higher than P_{Crit} and to the left of the "dome": the liquid region;
  to the right of T_{Crit}, for pressures below P_{Crit} and to the right of the "dome": and at any higher than P_{Crit} : the vapor region;
- the thermodynamic "dome" in which liquid➔ vapor and vapor➔ liquid phase transitions can occur. The dome is bounder on the left by the saturated liquid line, and on the right by the saturated vapor line.

Note: Above T_{Crit} the fluid is a vapour, no matter what pressure it is compressed to. It cannot be liquefied by compression.

Let's look at the thermodynamic loop, which proceeds as an anti-clockwise rotation. The thing to note is that phase change occurs at constant pressure and temperature in the region of the p-H diagram under the thermodynamic "dome" (where in figure 3.1 the isotherms are horizontal).

- In segment (**D➔A**): heat extraction (**enthalpy increase**) occurs through the progressive evaporation of liquid into vapour along the length of a serpentine tube (usually finned: the "evaporator") at -10 ˚C inside the refrigerator cold compartment;
- In segment (**A_1➔B**): the vapor exiting the evaporator heats a little as it enters the warm exterior and is then compressed mechanically, causing its temperature & pressure to increase significantly (to around 65 ˚C) through the application of mechanical work));
- In segment *(**B➔C**) the hot vapour cools a little then condenses (**enthalpy decrease)** at 40 ˚C in the hot radiator located behind the refrigerator cold compartment);*
- In segment *(**C_1➔D**) the liquid passes through a "detent" (**forced pressure drop at constant temperature and enthalpy**). It cools at constant enthalpy by a phenomenon known as Jouls-hompson cooling. The detent device through a throttling element like an orifice, valve or thin tube (capillary). The restriction in this device is intended to provide the necessary mass flow of refrigerant liquid for the required refrigerator power in Watts. Together with*

[1] ***Note:*** *R404A is a commonly-used refrigerant. It is blended from three Hydro-Fluoro-Carbon (HFC) refrigerants: (52% R143A ($C_2H_3F_3$) + 44% R125 (CF_3-CHF_2) + 4% R134A (CH_2F-CF_3)), and is intended to have similar thermodynamic properties the Chloro-Fluoro-Carbon (CFC) refrigerants R22 ($CHClF_2$) and R502 (CF_3 - $CClF_2$). Such CFC refrigerants are known to damage the Earth's ozone layer and have been banned for a number of years. Although non-ozone depleting, (HFC) refrigerants however have high global warming potentials and are also being progressively phased out.*

the compressor's own compression ratio the restriction (liquid pressure drop (bars) for a required mass flow rate (kg.s^{-1})) helps to define the condensation pressure.

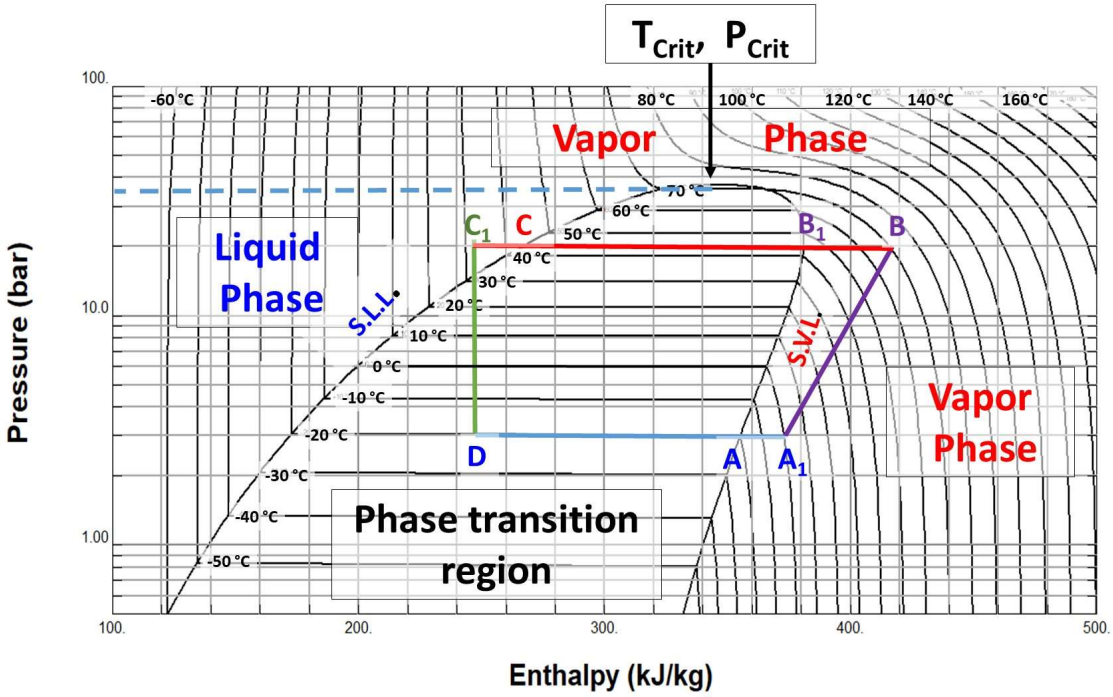

Fig 3.1: Pressure-enthalpy diagram: example: *for a domestic refrigerator closed-loop cycle with R404A refrigerant: (**D➔A**): heat extraction (**enthalpy increase**) - evaporation at -20 ˚C; (**A$_1$➔B**) vapour compression (**temperature & pressure increase through mechanical work)**), (**B➔C**) condensation (**enthalpy decrease)** at 43 ˚C (hot condenser radiator of refrigerator); (**C$_1$➔D**) liquid "detent" (**Joule-Thompson cooling through forced pressure drop at constant enthalpy**) through a throttling element like an orifice, valve or thin tube (capillary).*
***P-h** diagram calculated with [3.1].*

Looking at path ***(D➔A)***: in fig. 3.1 at -20 ˚C we see that the difference in enthalpy necessary to evaporate 1 kg of R404A is the difference between points **D** (360 kJ.kg^{-1}) & **A** (245 kJ.kg^{-1}) referred to the horizontal enthalpy axis. This ***enthalpy difference*** of 115 kJ.kg^{-1} tells us the refrigerative (here evaporative) power ***ERP$_{P,T}$* (W)** that a mass flow of 1 kg.s^{-1} of this fluid can remove at these conditions of (constant) temperature and pressure, as follows:

Evaporative Refrigerative power ***ERP*** (in Watts) can be expressed as:

$$ERP = \delta H_{P,T} * \dot{m} \qquad (3.2)$$

where $\dot{m}$ is the mass flow in kg.s^{-1}

The mass flow $\dot{m}$ of refrigerant necessary for required refrigerative power ***ERP*** is thus:

$$\dot{m} = ERP / \delta H_{P,T} \qquad (3.3)$$

As an example, a domestic refrigerator needs to evaporate 2.6.10^{-3} kg.s^{-1} or 2.6 grams per second of R404A for an evaporative refrigerative power of 300 Watts in the conditions of transition ***D➔A*** of fig 3.1.

In a domestic refrigerator this quantity of vapour must now be dealt with: energy has been extracted from liquid R404A in the path ***D➔A*** and somewhere - for conservation of energy in

a closed system - it must be re-supplied or 'repaid'. This is done by applying mechanical work to the vapor using a compressor as shown in fig. 3.2, increasing the pressure from 3 bar to 18 bar (path ***A_1 → B***). In doing this, the vapour heats from -20 ˚C to about 70 ˚C (at the output of the compressor).

From the compressor the vapour passes through the condenser radiator on the back of the refrigerator, cooling as it does so ***(***path ***B → C). There is again an enthalpy change: a reduction from around 410*** kJ.kg^{-1} ***to around 260*** kJ.kg^{-1}***. Not all this enthalpy change is dedicated to*** condensation: the vapour cools from about 70 ˚C (compressor casing and output tube coupling) to 43˚C before the condensation starts at point **B_1**, where the corresponding enthalpy is 380 kJ.kg$^{-1.}$ The enthalpy change due to condensation alone is therefore about 120 kJ.kg^{-1}, which is about the same as the enthalpy difference for evaporation.

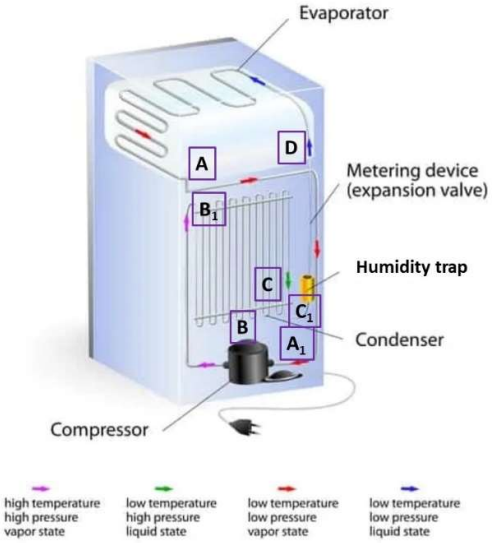

Fig 3.2: *Main components of a domestic refrigerator operating in a closed-loop cycle. The indices correspond to those of the R404A thermodynamic cycle shown in fig. 3.1.*
*(**D → A**): heat extraction (evaporation of liquid at -10 ˚C) in the internal compartment;*
*(**A_1 → B**) compression of vapour (**temperature & pressure increase)** followed by*
*(**B → C**) condensation at 40 ˚C (hot radiator behind the refrigerator);*
*(**C_1 → D**) liquid "detent" (**forced pressure drop at constant enthalpy**) through a Joule-Thompson throttling element like (orifice, expansion valve (fig. 1.5) or thin tube (capillary)).*

A thermodynamic cycle such as that shown in fig. 3.1 can be represented in a different way, as in fig 3.3. In fig 3.3 the "fluid" can be thought of sand which must be picked up (in analogy with evaporation), by a digger (the "system"), which then carries the sand up to a higher potential energy (in analogy with compression), then dumps it onto a higher platform (in analogy with condensation) from where it can fall through a narrow trapdoor to the lower level again, losing that acquired potential energy (in analogy with liquid detent). Energy is consumed by the system in terms of the diesel used to move the digger and lift its bucket. Figure 3.3 illustrates this analogy in the context of the cooling system of the ATLAS silicon tracker [3.2] at the CERN Large Hadron Collider, which evacuates around 60kW of heat using the evaporation of octafluoropropane (C_3F_8). The cycle shown in fig. 3.3, like that of fig. 3.1, is a compressive cycle with rotation in an anticlockwise direction on the p-h diagram. Condensation occurs at a higher pressure and temperature than evaporation (as in a domestic

refrigerator). We will see that rotation in the opposite clockwise direction is also possible: and also much more interesting!

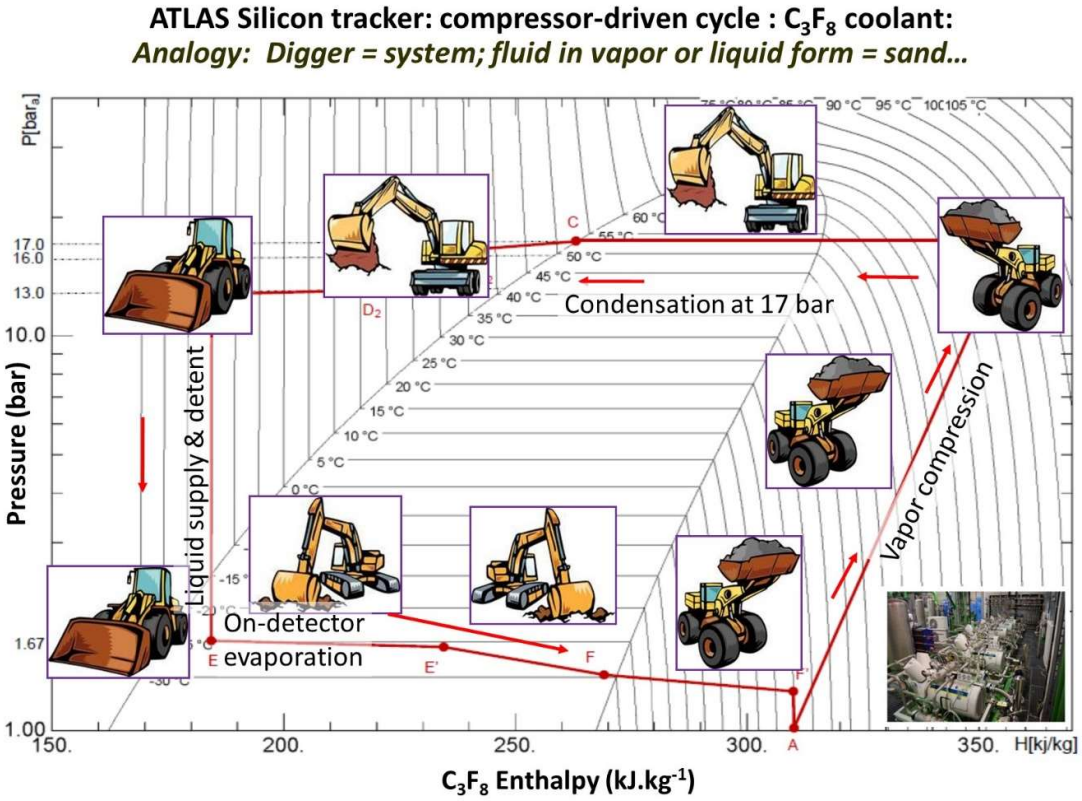

Fig. 3.3: *The "digger – sand" analogy in the context of the p-h diagram for the compressor-driven C_3F_8 (octafluoropropane) 60 kW evaporative cooling system of the ATLAS silicon tracker at the CERN Large Hadron Collider* [3.2]

Figures 3.4 and 3.5 illustrate elements of the Silicon tracker of the ATLAS experiment at the CERN Large Hadron Collider cooled by the evaporation of octafluoro-propane (C_3F_8). The tracker consists of 7 horizontal concentric "barrel" layers of silicon pixel and microstrip semiconductor detectors and 7 disks at each end to close off the "can" surrounding the proton-proton collision point at LHC "point 1". In addition to the evaporators shown in fig. 3.4 and the compressors other flow and pressure control elements include pressure regulators (for tuning liquid flow in individual circuits), capillaries of several metres length (for isothermal liquid pressure drop) and back pressure regulators for setting the evaporation pressure (and temperature in individual cooling circuits). The index points of fig. 3.5 correspond to those on the thermodynamic cycle diagram of fig. 3.3.

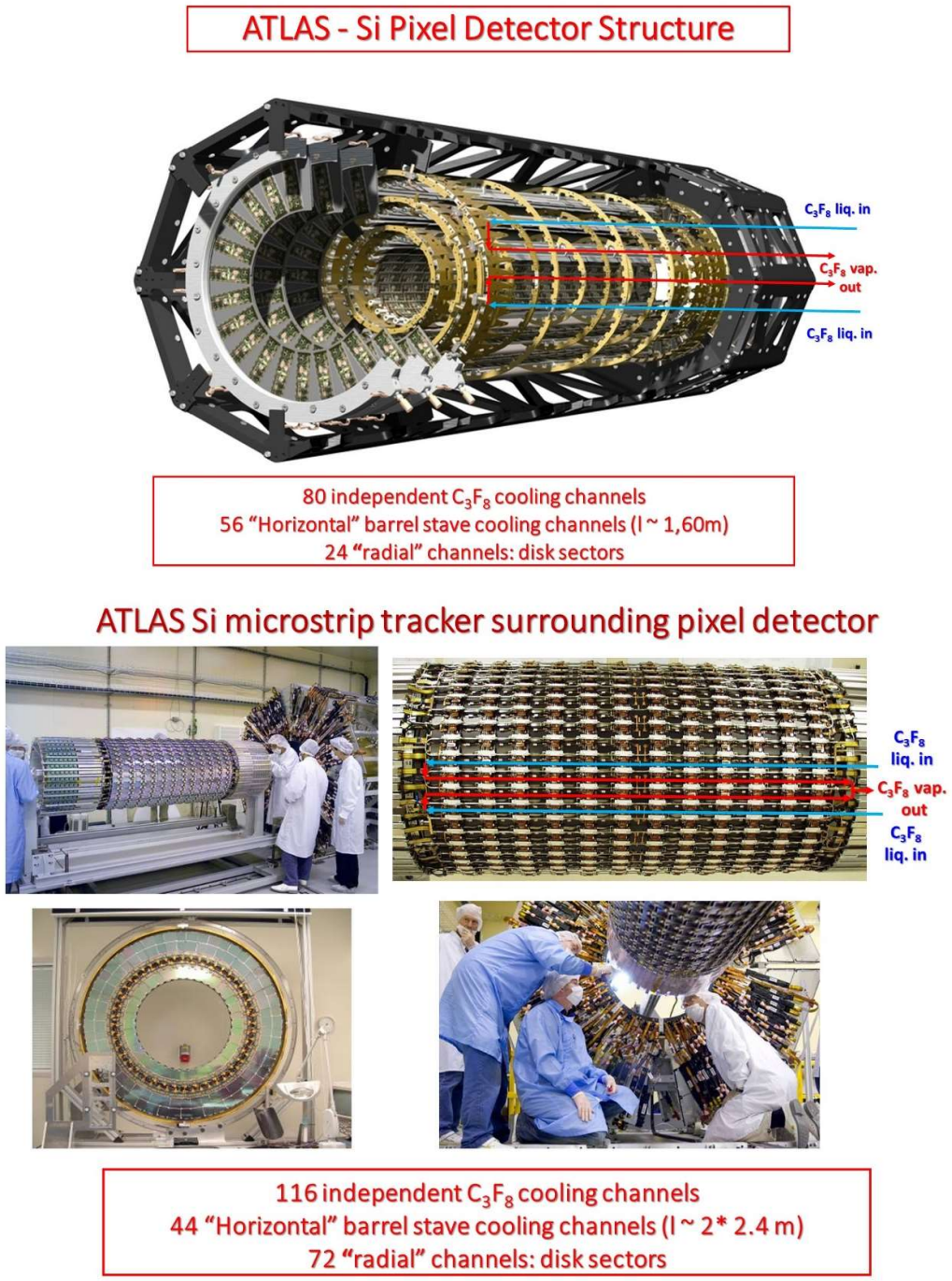

Fig 3.4: upper: *view of the ATLAS silicon pixel tracker, showing barrel and end-cap disk elements, and the on-detector (evaporator) flow path for C_3F_8 evaporative coolant.* ***lower:*** *views of major components of the ATLAS silicon microstrip tracker, showing barrel and end-cap disk elements, and the on-detector (evaporator) flow path for C_3F_8 evaporative coolant through the "block and tube" module attachment system.*

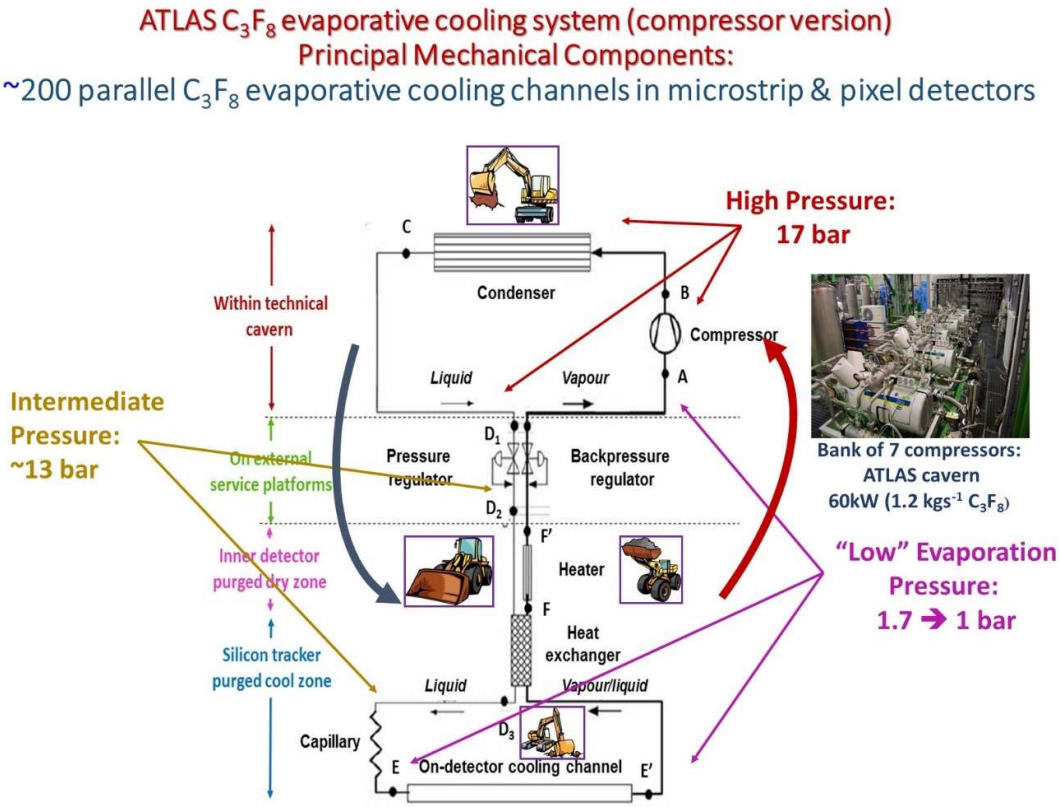

Fig 3.5: *Principal components of the compressor-driven version of the ATLAS C_3F_8 evaporative cooling system [3.2], including the on-detector evaporators, compressors, high pressure condenser tank, flow regulators and liquid delivery capillaries. Flow and pressure control elements for individual circuits include pressure regulators (liquid flow), and back pressure regulators (evaporation temperature). Index points correspond to those on the thermodynamic cycle diagram of fig 3.3.*

(3.3) A closed-loop thermodynamic cycle with "reverse" rotation (LHC-ATLAS thermosiphon)

Figures 3.6 – 3.9 illustrate the ATLAS Thermosiphon-based cooling system [3.3] that replaced the compressor driven system in 2018. The compressor system is now the back-up and automatic changeovers can be made between the two systems. The difference in the thermosiphon is that the 17 bars of pressure necessary to drive liquid C_3F_8 through the ATLAS silicon tracker cooling (which has around 200 independent cooling channels) is generated by the $\rho.g.h$ hydrostatic column of 92 metres of liquid C_3F_8: due mainly to the depth of the ATLAS detector below ground in its subterranean cavern.

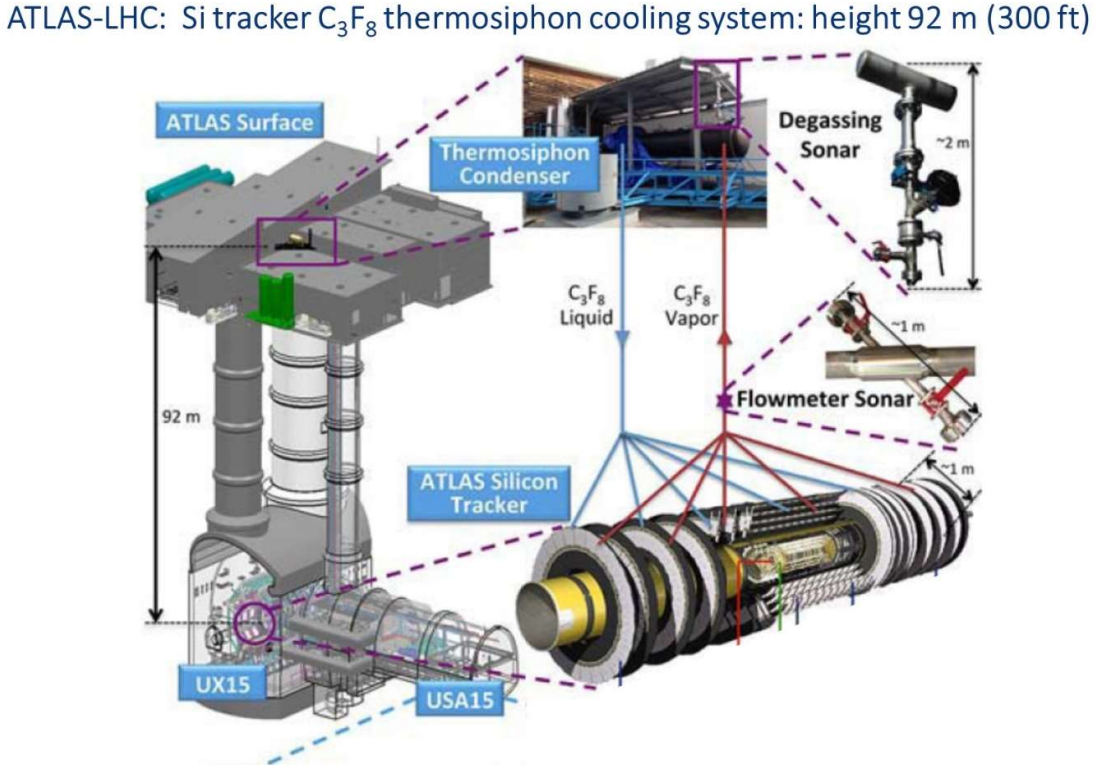

Fig 3.6*: The layout of the ATLAS thermosiphon C_3F_8 evaporative cooling system, showing the components at elevated level, ground level and below ground.*

The condenser (illustrated in figs 3.8 & 3.9) is both the highest and the coldest part of the thermosiphon system: and is cooled to -65 ˚C with the use of a chilled intermediate C_6F_{14} (perfluoro-n-hexane, FC-72) cooling fluid (or "brine" – the commonly-used name for any transfer fluid with a freezing point lower than water: in the case of C_6F_{14} it is around -100 ˚C). C_3F_8 is condensed at the rate of about 1.2 $kg.s^{-1}$.To do this a very high mass flow of C_6F_{14} is needed, provided by the powerful pumps of the ground-level cooling plant shown in fig. 3.7. This flow rate difference is another manifestation of the performance difference in uniphase and phase-changing latent heat (or enthalpy) cooling systems. Figures 3.6 & 3.7 illustrate the major components of the ATLAS thermosiphon and their placement at LHC point 1, and of the condenser in particular.

Fig 3.7: *Main components of the ATLAS thermosiphon C_3F_8 evaporative cooling system, with their locations at elevated level, ground level and below ground.*

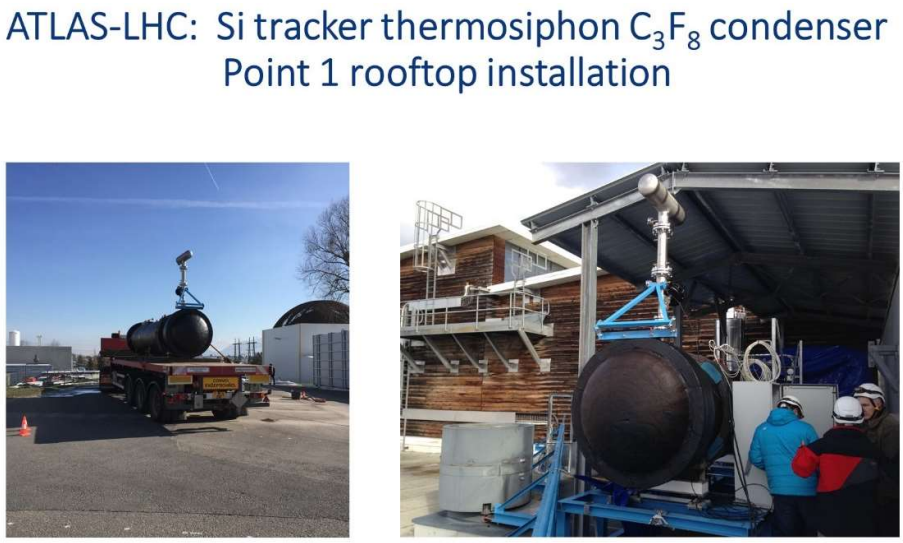

Fig 3.8: *Installation of the condenser of the ATLAS thermospiphon on the roof of the CERN LHC Point 1 facilities building (15 meters above ground level, 92 meters above the ATLAS experimental cavern).*

Figure 3.9 illustrates the condenser internal construction. In the "U-tube" heat exchanger geometry. C_6F_{14} flows through more than 310 longitudinal tube runs while C_3F_8 vapor enters the space around them, condensing on their cold surface and collecting in the bottom 1/3 of the cylinder, where it is kept cold ("sub-cooled") by further tubes with C_6F_{14} flowing. The ratio of the numbers of tubes used in condensation (around 90% of the total) reflects the much higher refrigerative power needed to condense the C_3F_8 (a bi-phase change) than to keep it cold – a uniphase exchange.)

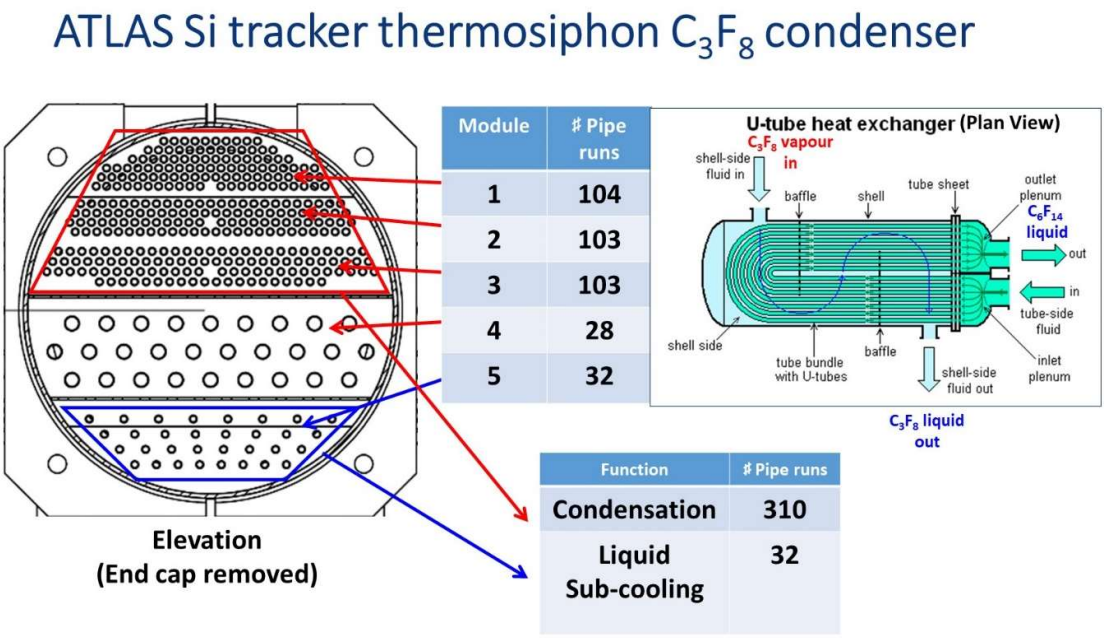

Fig. 3.9: *Internal construction of the ATLAS thermosiphon C_3F_8 condenser.*

Figure 3.10 shows the ***p-h*** diagram for the ATLAS thermosiphon system, with the digger-sand analogy model superimposed. It can be seen that the rotation on the thermodynamic diagram is now clockwise, because the condenser is now colder than the evaporator. In fact everything happening in the primary C_3F_8 evaporative circuit which cools the silicon tracker is now entirely passive (apart from remote-controlled valves and regulators), with no large reciprocating components like the pistons of compressors. The elimination of vibration in this way has improved the leak-tightness of the C_3F_8 cooling system; an important consideration as this fluid has a high global warming potential [see section 7]. Figure 3.10a shows the ***p-h*** diagram for the system with the digger-sand analogy model superimposed, while fig. 10b shows the C_3F_8 pressure-enthalpy diagram with the thermodynamic 'waypoints' (➔L➔M➔N➔O➔A➔B➔C➔D➔E➔F➔G➔H➔I➔J➔K➔) superimposed on the thermosiphon piping schematic diagram.

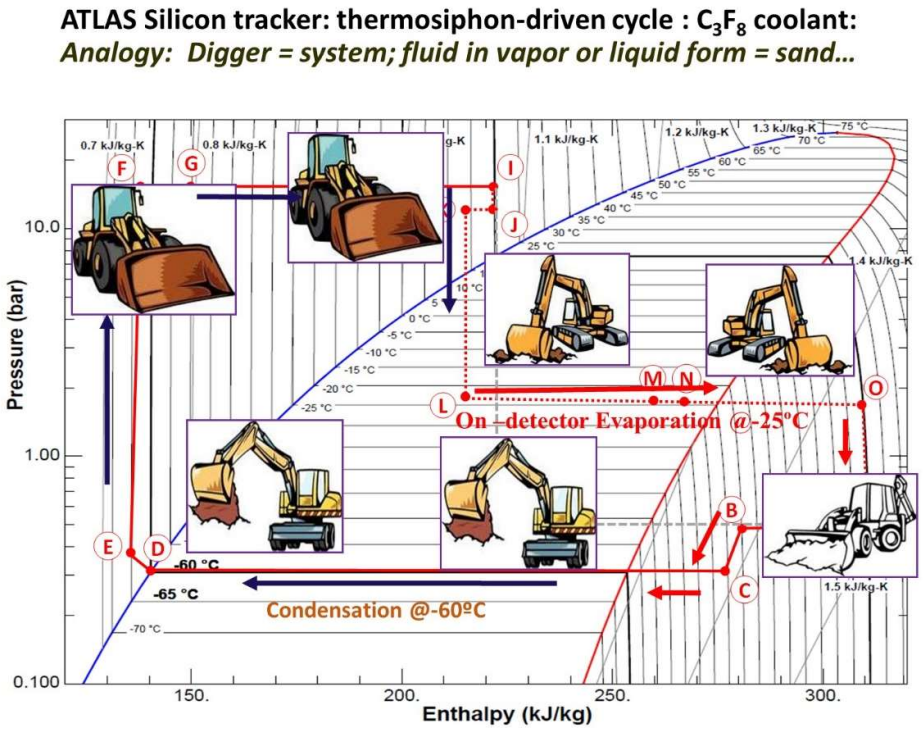

Fig. 3.10a: *The "digger – sand" analogy in the context of the p-h diagram for the thermosiphon-driven C_3F_8 (octafluoropropane) 60 kW evaporative cooling system of the ATLAS silicon tracker at the CERN Large Hadron Collider [3.3]*

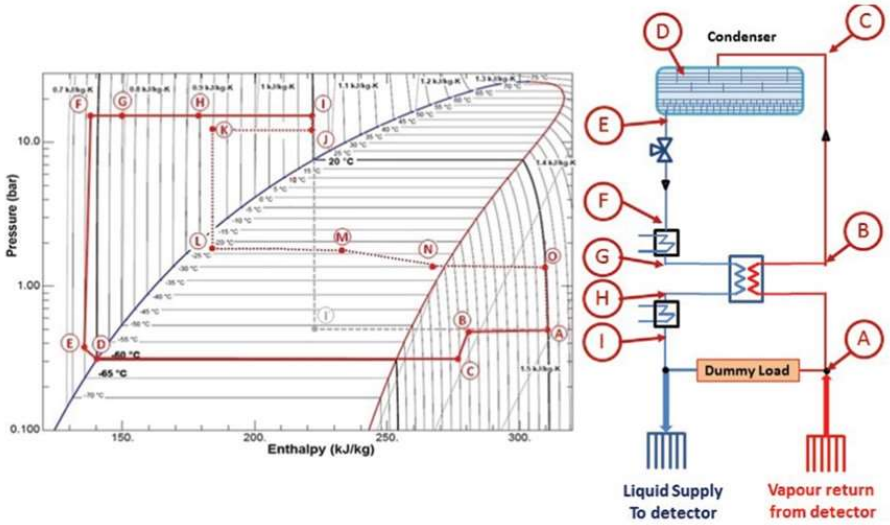

Fig. 3.10b: *C_3F_8 pressure-enthalpy diagram with the thermodynamic 'waypoints' (➔L ➔… ➔K ➔) superimposed on the thermosiphon piping schematic diagram.*

Fig. 10b: C_3F_8 pressure-enthalpy diagram with the thermodynamic 'waypoints' ➔L➔..,➔K➔ superimposed on the thermosiphon equipment diagram.

Problem (3.1) see also separate sheet:

From Fig. 3.9 it was clear that a large number of tubes are needed to condense approximately 1.2 kgs-1 of C_3F_8 to cool the ATLAS silicon tracker. This implies that a high mass flow of C_6F_{14} liquid is needed, but what this mass flow (kg.s-1)?

Hints to solve this problem:

- Looking at figure 3.10 we see that considerable thermal energy has to be extracted from the C_3F_8 vapor to reduce its temperature from around 20 ˚C (the temperature acquired in traveling through more than 92 meters of pipes to the condenser) to -60 ˚C, where phase change can occur under the "dome";
- Some of this heat is extracted from the vapour at a C_3F_8 pressure of 320 mbar within the condenser itself (using a counter-flow of cold C_6F_{14}), cooling the vapor from -25 ˚C (point **C**) to -60 ˚C before the vapour begins to condense at the saturated vapour boundary of the dome.
- Moving left from the saturated vapour boundary of the dome all energy goes into condensing the C_3F_8.
- You should therefore use the entire **CD** enthalpy difference in your calculation, and only this;
- The specific heat capacity of C_6F_{14} in the range -60 ➔ -65 ˚C is around 925 $J.kg^{-1}$. C_6F_{14} remains a liquid and does not change phase during this process, but heats up by 5 ˚C.

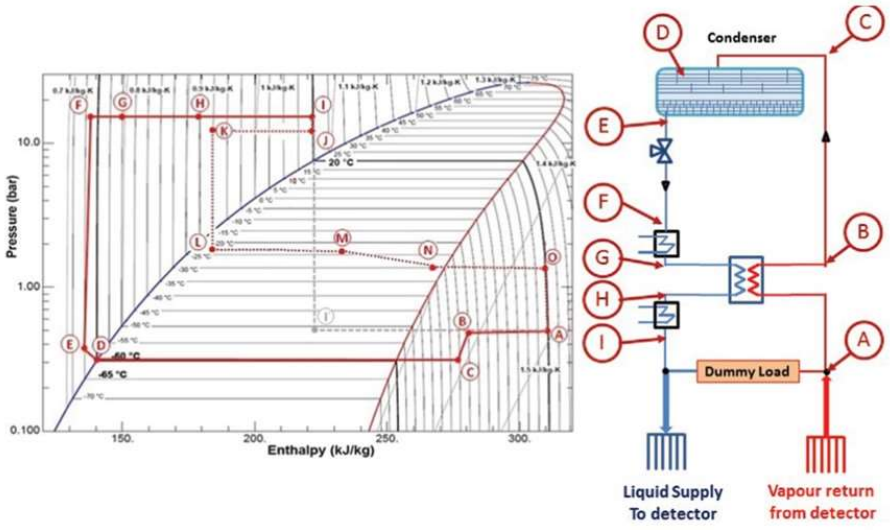

(3.4) The Heat Pipe

Heat pipes (for a typical reference see [3.4]) are hollow tubes (usually copper) containing a volatile fluid which evaporates at the "hot" end and flows as vapour to the cold end where it condenses, giving up its heat acquired in evaporation. The tube wall may be equipped with internal grooves through which the condensed fluid flows by capillarity back towards the hot end. In other implementations, a sintered (deposited, amorphous) metallic "wick" may be deposited on the inside of the tube wall to as the liquid conduit. Fig 3.11 illustrates the action of a heat pipe. Heat pipes thus have their own internal atmospheres and "micro climates". These devices are now ubiquitous in the cooling of computer cores, in both desktop and laptop and Graphical Processor Units.

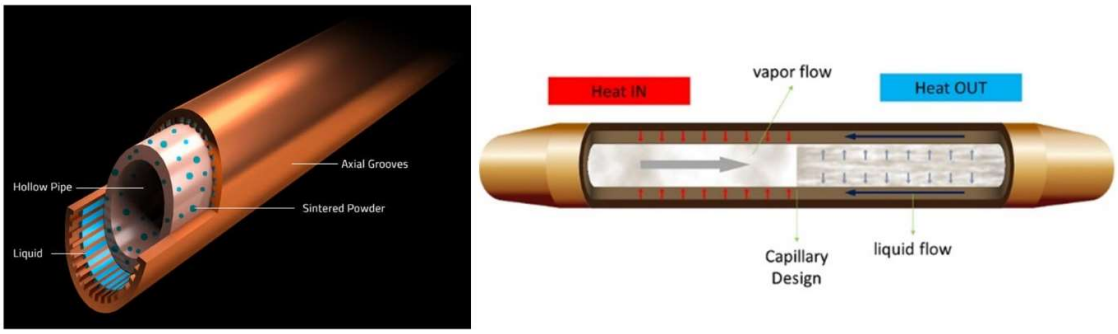

Fig. 3.11*: Principle of operation of a heat pipe*

Figure 3.12 illustrates heat pipes configured for installation in laptop and desktop geometries. The "hot" ends of the heat pipes are held (usually clamped) in contact with the processor to be cooled. They may be flattened to increase their contact area. In low profile geometries they may be flattened over their entire length. The use of several heat pipes also allows for redundancy. The cold ends of the heat pipes usually enter some kind of finned radiator to increase the contact area with the air flow driven by a fan. The fan operates at low voltage (typically less than 12V) and is started and stopped with feedback from a temperature sensor. The fan may be driven by pulse width modulation or by an analog DC voltage, ideally using an embedded PID algorithm. Numerous add-on fan-apps are available, and (multiple) fan control is a subject of great interest in the overclocking community. Heat pipes can, of course, also be used to conduct heat to liquid-cooled heat exchangers.

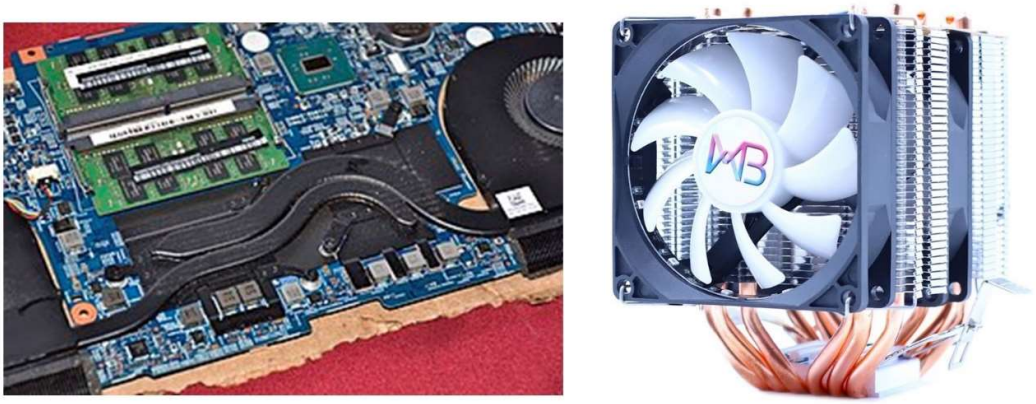

Fig. 3.12: *Left: typical heat pipe installation in a laptop or server (low profile) geometry machine, intended to channel the heat to a radiator and ventilation fan:*
Right: typical heat pipe installation for a desktop, with less stringent space constraints.

For normal room temperature operation demineralized water is a convenient heat pipe working fluid due to its extremely high latent heat, or enthalpy, of evaporation (around 2.5 $MJ.kg^{-1}$!!). However very low pressure operation (in the range of a few mbar) is necessary, with a charge of a fraction of a gramme of water injected into a typical computer application heat pipe. This in turn requires long-term hermeticity against air ingress. For lower temperature applications, ammonia, acetone and methanol are used. The thermal conductivity of a heat pipe used in electronics cooling applications can be in the range 1500-50000 $W.m^{-1}.K^{-1}$, far exceeding the thermal conductivity of solid copper (390 $Wm^{-1}K^{-1}$).

Problem (3.2) see also separate sheet:

A processor chip dissipating 75W needs to be cooled by conducting heat away to a finned heat exchanger (the heat sink). The cooling block in contact with the chip through a thin thermal grease joint has grooves for three 6 mm diameter heat conduits, as shown in the figure. The total cooling path from the center of the cooling block to the center of the finned radiator is 15 cm. The fan is powerful enough (and has enough range of driving voltage) to keep the heat sink at 40˚ C under all circumstances. This temperature is maintained by feedback from a temperature sensor mounted near the fan itself (note the 4-wire connector in the photo montage).

The computer user notices that, after turn-on the processor chip (monitored by its own internal temperature sensor) rapidly increases to over 12 ˚C higher than its normal operating temperature before the system annoyingly takes remedial action by decreasing the processor clock frequency etc. Doing some research the user finds that this cooling configuration uses three low-pressure water-filled copper heat pipes with 1mm wall thickness and a nominal thermal conductivity 20000 $W.m^{-1}.K^{-1}$ and surmises that one might have failed (leaked up to atmospheric pressure).

- Would the user be correct in this assumption?
- Why, or why not? Show your reasoning with a calculation.

Hint: a failed heat pipe would revert to the thermal conductivity of a copper tube of 6mm outer diameter and 1mm wall thickness.

(3.5) Phase change cooling (ice melting), latent heat of melting of fusion (CODE "P": measurement in water system)

Remembering fig 2.4…

Though something like this could easily sink the Titanic, this is like a minnow compared to a whale in terms of the ice loss problem, as we shall see. An ecological problem …

Problem (3.3): see also separate sheet.

Part of the Larsen-C ice shelf broke off from Antarctica in July 2017 and drifted North as iceberg A-68 before melting away. A-68 was 170 km long, 50 km wide with an average thickness of 200m.

(a) Using the Latent heat of fusion ***L*** of water (333 $kJ.kg^{-1}$) estimate the combined energy absorbed from the sea and atmosphere to melt A-68.

(b) Let's assume that the energy from (a) comes from global warming.
It is estimated (with big uncertainties as inspections are less frequent than they used to be) that the World's stockpile of nuclear weapons is around 10 000 megatonnes of TNT equivalent. The explosion of 1 megatonne of TNT has an energy release of around $4.2.10^{15}$ Joules. What percentage of the World's 10000 Mt stockpile of nuclear weapons would need to be exploded to melt iceberg A-68? (Assume all the energy goes into melting ice). How many gigajoules is that?

(c) Now let's pretend that A-68 never existed (i.e. that there is no ice to buffer atmospheric heating), and that the global warming energy calculated from (a) above went instead into heating the Earth's atmosphere. Taking the Earth's radius as 6370 km and assuming the effective atmospheric depth to be 16 km (this height contains more than 90% of the atmospheric mass), how much would the atmospheric mass be raised in temperature?

(d) Should we be worried? Why, or why not?

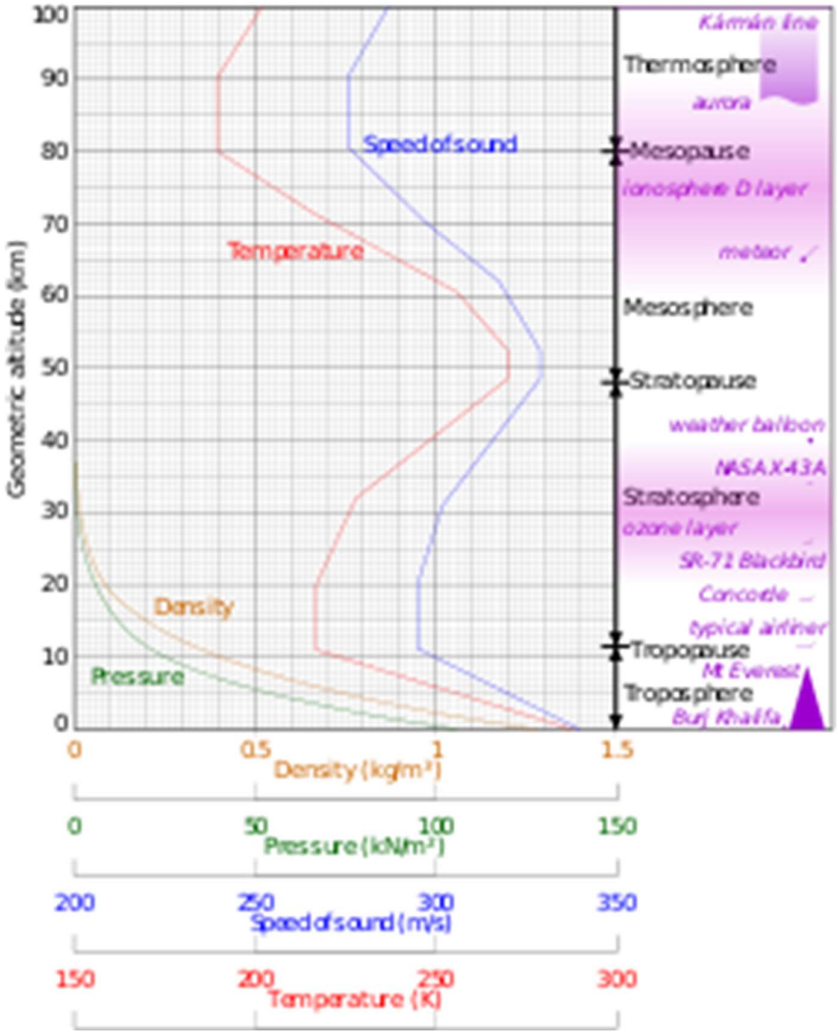

Hints

(1) use "average values" of the ***Cp*** (1.0036 $kJ.kg^{-1}.K^{-1}$) and density of air (0.45 $kg.m^{-3}$) [3.1] at the temperature of – 43˚C and pressure (0.3 bar_{abs}) [3.5] , corresponding to an altitude of 8 km: half the 90% mass height of 16 km;

(2) The average sea depth is 3688 metres and sea covers 71% of the Earth's surface. Oceans hold 96.5% of the Earth's water. According to the U.S. Geological Survey, there are over 1,386,000,000 cubic kilometers of water on the planet. Of this vast volume NOAA's National Geophysical Data Center estimates that 1,335,000,000 cubic kilometers is in the oceans. Ocean water mass = 1.335. 10^{18} tonnes.

(4) Peltier Thermo-electric Cooling Devices (Code I)

Peltier cooling devices [4.1] exploit the thermoelectric effect of dissimilar metals or semiconductors. Just as a temperature change applied to a junction of two dissimilar metals can generate a measureable voltage, passing an electric current through a bi-metallic junction can generate a temperature gradient. This effect, the Seebeck effect, is exploited in solid-state Peltier cooling elements, which can be bought inexpensively in dimensions adapted to processor chip cooling applications.

Figure 4.1 illustrates a typical Peltier thermoelectric cooling (TEC) device. Such devices have a descriptor printed on the cooled (or heat absorbing) side, indicating the number of stages, number of semiconductor "couples" and the current rating in amperes. The common and inexpensive *TEC1-12706* variant (shown) with (40 x 40 mm) square thermal contact surface and a depth of $3-4$ mm can transport around 60 W of heat for a typical DC voltage of around 12 V and current of 6 A (resistance $2\ \Omega$).

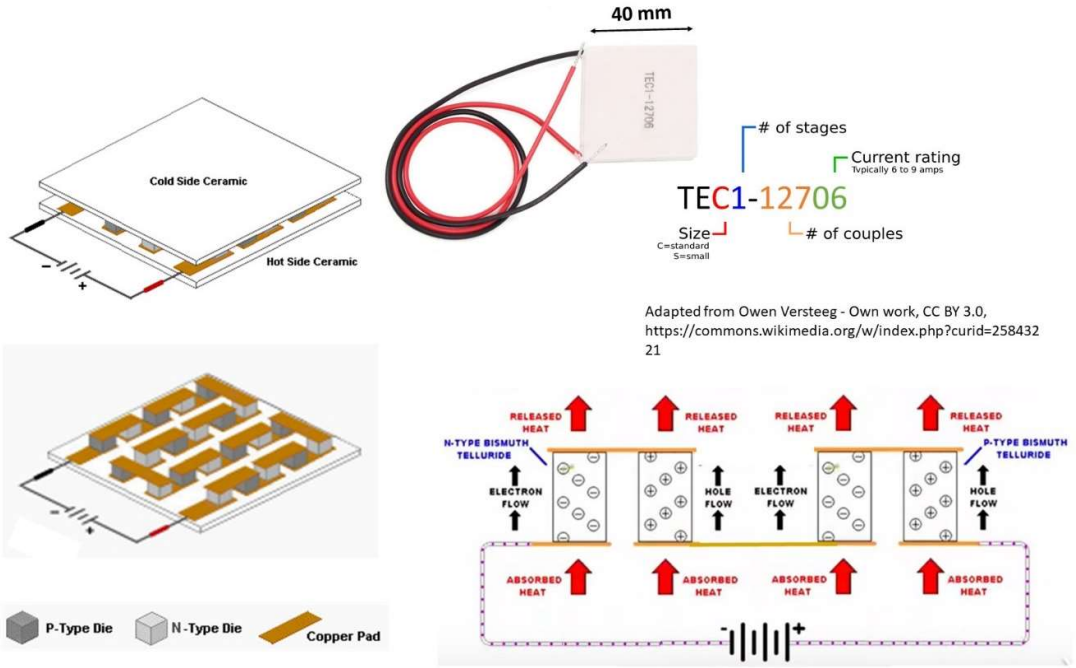

Fig. 4.1: *Construction of a Peltier thermoelectric cooling module showing the internal series attachment of the semiconductor "couples" and the flow of heat through the device. Vignettes adapted mainly from Wikipedia reference [4.1].*

Figure 4.1 illustrates the internal construction of a typical TEC. Two alumina ceramic substrates "sandwich" many pairs, or "couples", of (for example) Bismuth Telluride (Bi_2Te_3) semiconductor dies which are connected through copper pads in series in an alternating n-doped (electron rich) and p-doped (electron deficient) sequence. The couples are mechanically constrained to be thermally in parallel, forming heat-conducting "columns" between (electrically-insulating) ceramic plates, with heat transferred through the columns by the majority charge carriers (electrons in n-type Bi_2Te_3, holes in p-type) with no moving parts. The current flowing through the series die circuit naturally configures for all couples:

(a) *the more +ve voltage contact onto p-type* (and the *more -ve voltage* contact onto n-type) material as heat absorbing junctions;
(b) the more *-ve voltage contacts onto p-type* (and the *more +ve voltage* contacts onto n-type) material as heat emitting junctions to be coupled to a cold thermal drain.

Since junctions of type (a) are all at the same temperature (as are those of type (b), in contact with the other alumina plate) the absorptive side ***of a thermally disconnected TEC*** would become colder from the contributions of all the couples, while the emissive side would become correspondingly hotter.

The necessary internal gaps create a "void fraction" between the columns, reducing the available thermal conductivity for a given surface area relative to a monolithic material. Peltier devices are reversible and variable in their heat transfer, according to the polarity and magnitude of the current applied. Typical offsets of 60 ˚C are possible in 12 Volt, 6A devices. Bismuth Telluride remains the most economical material for TECs in ambient temperature applications. However, at low temperatures (around -110 ˚C) its semiconducting properties diminish.

In a typical processor cooling configuration the emissive side of the TEC is attached to a heat sink, which may be water-cooled or (more usually) finned and fan-cooled, while the absorptive side is attached to the processor core through a thermally-conducting paste. In some applications, multiple coolers may be cascaded to achieve a greater thermal difference between the load and the heatsink, but this often comes at the expense of reduced efficiency or *Coefficient of Performance* (COP): the extra paste interfaces between the ceramic plates of the cascaded TECs will introduce discontinuities in thermal conductivity for example.

The power in Watts, **Q,** that can be moved by a TEC device is proportional to the current, ***I***, and the temperature-dependent Peltier coefficient of the material, ***P***, expressed in volts:'

$$Q = P.I \tag{4.1}$$

The Peltier coefficient depends on temperature and the TEC material choice. Below -110 ˚C, for example, the semiconducting properties of Bi_2Te_3 diminish. Peltier coefficients of 10 $W.A^{-1}$ are common, but are offset by two phenomena:

- parasitic heat $\boldsymbol{Q_P}$ (Watts) *due to resistive self-heating:*

$$Q_P = I^2.r \tag{4.2}$$

where ***r*** is the resistance of the series couples circuit;

- the heat flux from the hot (emissive) side to the cool (absorptive) by conduction through the columnar structure of the couples. This heat is in the opposite direction to the extraction direction of the TEC itself, and subtracts more from its efficiency as the temperature difference grows. A single-stage thermoelectric cooler can typically produce a maximum temperature difference of 70 °C between its hot and cold sides.

In refrigeration applications TEC devices have an efficiency of 10-15%, compared with 40–60% achieved in phase change systems. As a result, thermoelectric cooling is normally used in environments where the compact, solid-state nature (low maintenance through no moving parts) and insensitivity to orientation outweigh efficiency considerations.

Figure 4.2 shows the ultimate do-it-yourself cooling kit (around $60 on Amazon.com) for the user who is not quite sure what cooling combo to use for their processor chip: liquid?

Peltier? Heat pipes? Fins? Fans? Not very compact, and in other orientations other than the horizontal shown it would probably pull the chip out of the motherboard ;) ! The kit doesn't seem to address direct evaporative cooling of electronic chips, but we looked at that in section 3 and will do so again in sections 6 & 7.

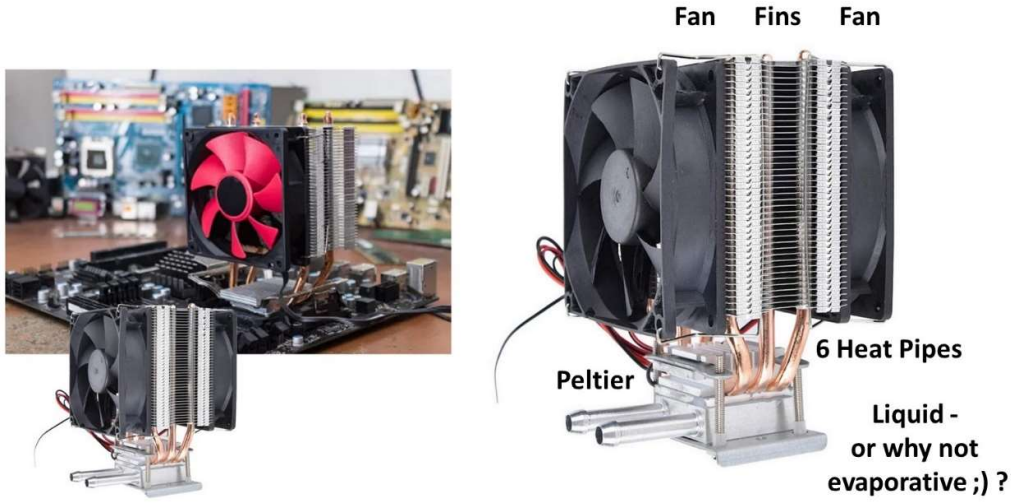

Fig. 4.2*: the (almost) ultimate do-it-yourself processor chip cooling kit: liquid? Peltier? heat pipes? fins? fans?*

(5) The Vortex tube: another (fairly extreme) example of Joule-Thomson Cooling:

Figure 5.1 illustrates a deceptively simple device - the "vortex tube" [5.1] (also known as a Ranque-Hilsch tube), that exploits the drop in temperature of a gas as it drops from a high pressure to a low pressure - for high flow gas cooling. In the device gas (usually filtered dry air) is injected tangentially at high pressure into a tube, creating an extremely fast vortex effect (up to a million rotations per minute). Gas spirals along the tube and is slowed down and compressed by a conical valve, exiting from one end of the device as hot gas. By contrast the heat exchange with the wave produced in return cools the gas reflected by the cone, which exits as cold gas at the opposite end of the device.

The opening around the outlet cone can be adjusted to vary the flow at the cold outlet: the greater the outlet flow, the lower the temperature. These devices are typically in dimensions of 10 to 40 cm in length and 1 to 5 cm in diameter, and can create a temperature difference of 70°C between the incoming gas and the cold exhaust. The gas consumption and noise generation of these devices can be very high (for example a device with a power of 85 (3000)W can have a gas consumption of 113 (4000!!) $l.min^{-1}$ and the gas atmosphere into which the chilled gas is injected must not itself condese (or have a condensible component) at the vortex tube cold gas output temperature. These devices are much less efficient in terms of energy (PV consumption) than conventional refrigerating units, but their low cost and simple installation make attractive for electronic rack cooling.

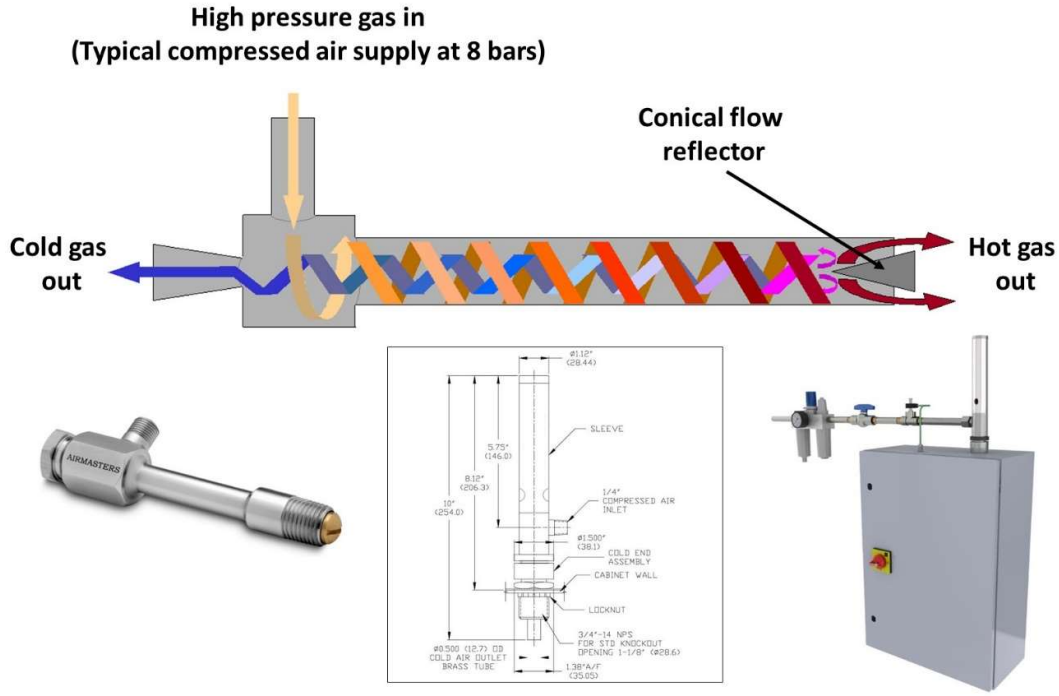

Fig. 5.1: *The "vortex tube" (or Ranque-Hilsch tube), showing the operating principle, dimensions of a typical device and an installation to cool an electronics cabinet.*

(6) Future implementation on a path to fully-integrated Silicon substrate cooling

At the very start of these course notes we saw *en-passant* an implementation of on-board (or nearly on-board) cooling of silicon pixel detector substrates for the **VE**rtex **LO**cator (VELO) detector of the LHCb experiment at the CERN LHC (fig. 6.1) [6.1].

In effect, the silicon pixel detectors and their readout electronics are ***almost directly*** cooled by fluid evaporating in microchannels. These microchannels (typically 200 x 120 microns) are not, however, etched in the silicon pixel detector (or the readout chips' own substrates), but into the heat collecting plates to which they are glued.

We can therefore ask:

- will processor chips ever have microchannels etched into them for direct coolant flow?
- will this coolant be liquid, or evaporative for reduced mass flow?
- how would the cooling pipes be connected?
- what would the (necessarily electrically non-conductive) fluid be: a fluorocarbon, CO_2 or a new low GWP fluid, for example from the 3M "NOVEC" range [6.2]?

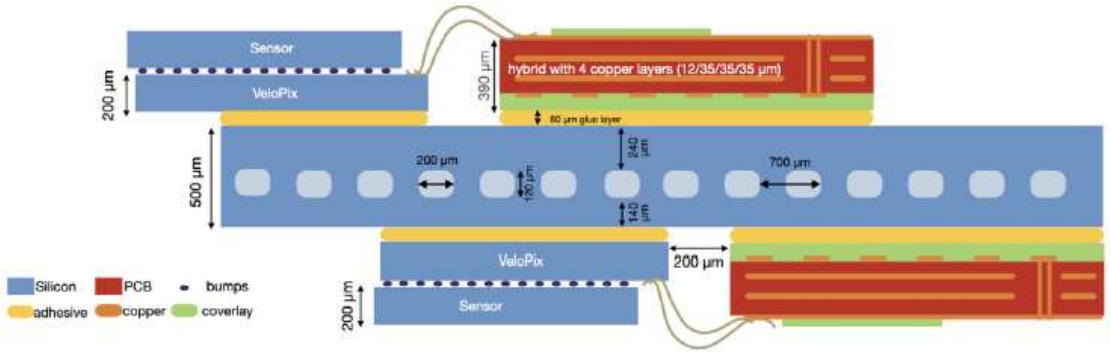

Fig. 6.1*: Micro-cooling channels etched in the heat collecting plates to which the silicon pixel detectors and front-end electronics of the* ***LHCb VE****rtex* ***LO****cator are glued.*

Figures 6.2 – 6.5 show other views of the LHCb VELO. This is the first detector to implement evaporative CO_2 cooling in microchannels. Extensive studies were needed [6.3] to characterise the evaporation of CO_2 in the channels and to verify that the channels, which comprise of top wafers bonded onto wafers with etched grooves, could tolerate the very high pressure of CO_2 evaporative cooling: which can be as high as 70 bars at room temperature (though following cool-down the pressure is lower, at around 18 bars at the operational evaporating temperature of -30 ˚C).

Evaporating CO_2 is a difficult fluid to circulate, particularly for cooling operations at room temperature - as in processor cooling - due to the high pressures that would be required. It is thus unlikely to hit the High Street, but there are other fluid possibilities with the necessary properties of non-conductivity, non-flammability, non-toxicity, with - as is becoming more important - low Global Warming Potential (GWP). We will see something about these developments in the next section, partly in the context of possible future use at CERN.

Fig. 6.2: *Framegrab from the CERN film (YouTube) on the LHCb VELO upgrade, showing the upgraded detector before its installation in LHC in 2022 [6.4], [6.5]*

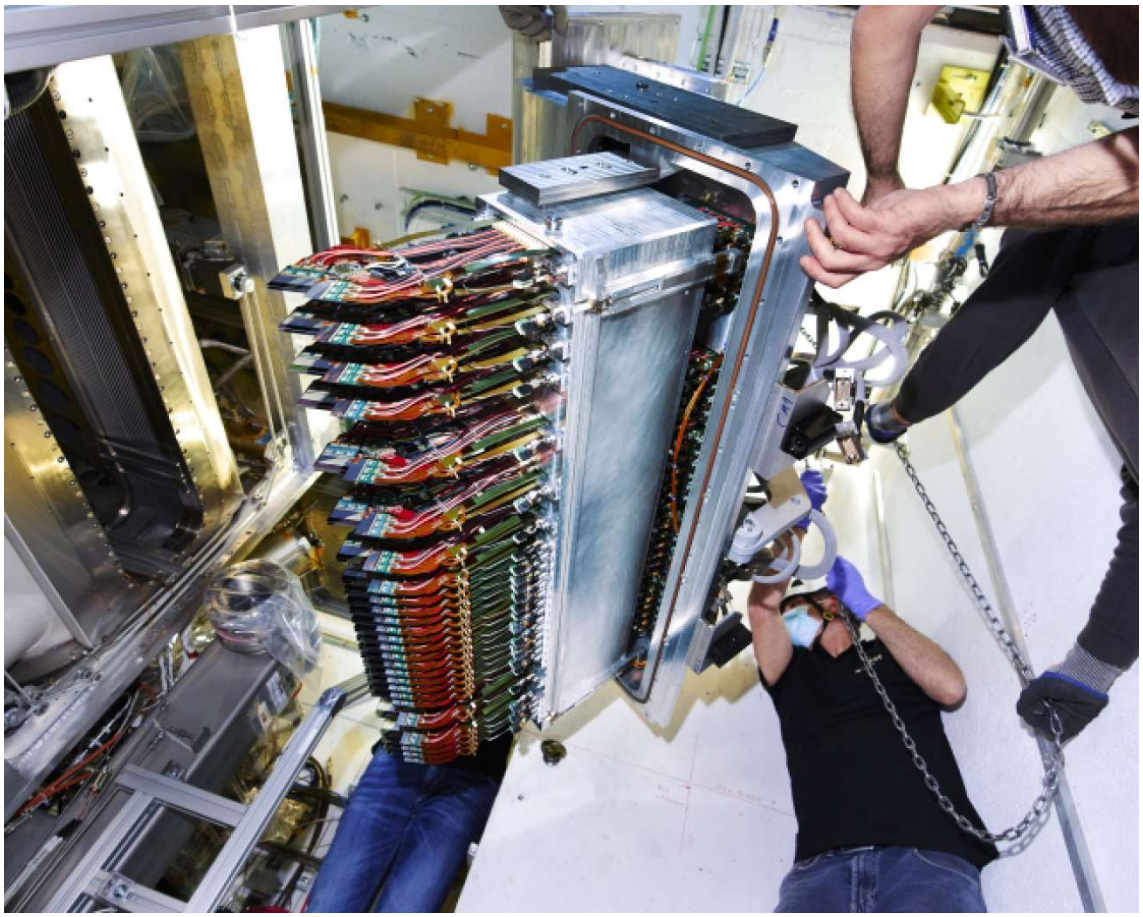

Fig. 6.3: The upgraded *LHCb VELO: preparation for final installation of the detector with its 52 pixel tracking elements into the LHC accelerator vacuum ring.*

Fig. 6.4: From the 2022 paper on the *LHCb VELO* upgrade*: detail of a pixel tracker elements and its microchannel heat extraction plate cooled by evaporating CO_2.*

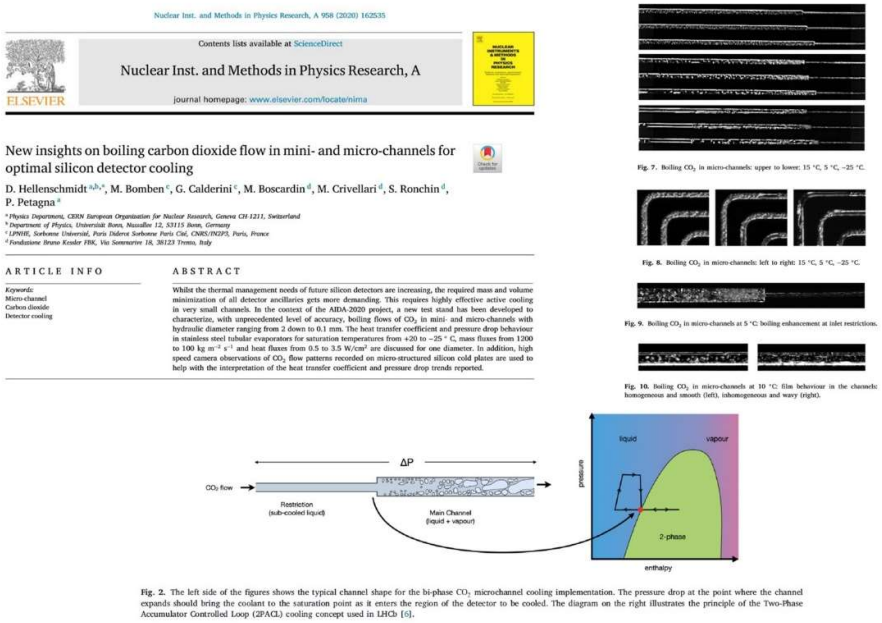

Fig. 6.5: From the 2020 study paper on CO_2 evaporation and evaporative flow patterns in narrow *microchannels. Bottom: detail of the on-board throttling device for each cooling channel: itself a preceding microchannel of smaller cross section.*

(7) Moving toward more environmentally refrigerants (Code I)

7.1 Silicon tracking detector cooling with fluorocarbons, CO_2 & fluoro-ketone fluids

Saturated fluorocarbons (***SFCs***) of the chemical form $C_nF_{(2n+2)}$, including 3M FC-77® used in the Cray-2 immersive cooling system (fig. 2.1)) have been used mainly in the electronics industry for more than 40 years. Many of these form the 3M range of Fluorinert® fluids [7.1] These uses include cooling and non-contact vapour-phase soldering in the manufacture of complex, dense printed circuit boards – a massive application. The non-conductivity, non-flammability and radiation-resistance of SFCs have also made them ideal coolant choices for detectors in particle physics experiments: C_6F_{14} (FC-72) is used as a liquid coolant for electronics in many sub-detectors at LHC experiments.

SFCs are non-flammable, non-toxic and (unlike many old, banned chloro-fluoro-carbon (CFC) refrigerants) non-ozone depleting. However have very high global warming potentials (GWP) - 5000-10000 times that of the same mass of CO_2. It is highly probable that their use will be restricted in the future, and the range of such fluids is shrinking. Despite this, the main moderators on restriction are the needs of the electronics industry and time needed for the development of alternatives.

Newer spur-oxygenated fluoro-ketones, for example from the 3M NOVEC® range [7.2], with chemical formulae of the form $C_nF_{2n}O$ can offer similar thermophysical performance to SFCs with but with extremely low, or zero, GWP. Although these fluids do not yet exist in large quantities over the full C_nF_{2n} "matrix" the radiation tolerance and thermal performance of NOVEC 649 ($C_6F_{12}O$) was sufficiently promising for it to be chosen by LHCb as a C_6F_{14} replacement for cooling silicon photomultipliers. [7.3], [7.4]. This fluid would also be a suitable replacement for C_6F_{14} in the CERN NA62 gigatracker, a pixel tracker using a liquid coolant circulating through microchannels [7.5].

Figure 7.1 compares the molecular shapes of a range of SFCs with spur-oxygenated fluoro-ketones of the same carbon order. The placement of the oxygen atom is critical to the molecular lifetime in the atmosphere and to its GWP: if the oxygen atom is placed on a spur these molecules suffer rapid scission in the intense UV environment of the upper atmosphere with the resulting debris molecules not having high GWP [7.6].

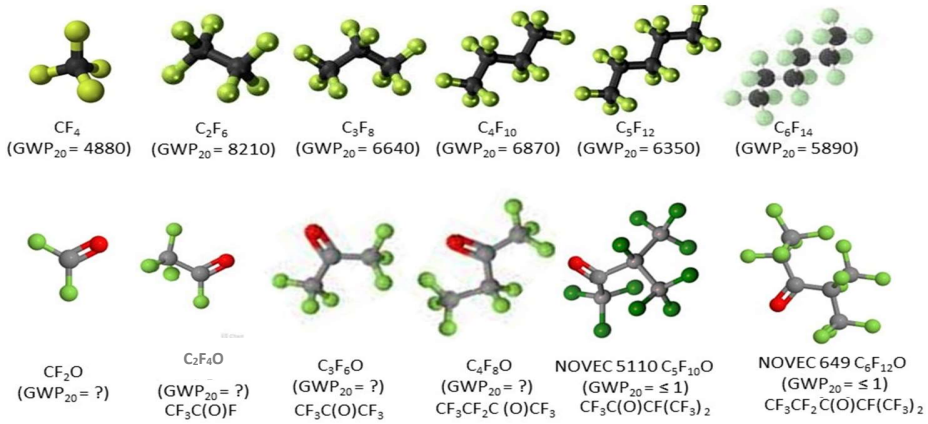

Fig 7.1: *molecular shapes of SFCs with same-order spur-oxygenated fluoro-ketones.*

7.1.1 Perspective from coolant use in current CERN silicon trackers

The primary (on-detector) cooling systems of the silicon trackers at LHC are currently based mainly on SFCs. Liquid C_6F_{14} cools the CMS silicon microstrip tracker [7.7] and the NA62 Gigatracker [7.5], while evaporative C_3F_8 cooling is used to cool the ATLAS SCT and pixel detectors [7.8,], [7.9]. The main cooling paramenters of most currently-operating CERN-based silicon tracking decetors are shown in table 7.1. Among these are the CO_2 evaporative systems that cool the CMS pixel detector [7.10], the ATLAS IBL ("Insertable B Layer") pixel detector [7.11] and the LHCb VELO [7.12]. In future upgrades to ATLAS and CMS it is planned to replace SFCs as far as possible with, for example, evaporative CO_2.

The trackers of table 7.1 are based on two main topologies (or types of "DNA"):

- **"tube and block"** geometry (in both barrel and end-cap disks, fig 3.4), with silicon detector modues attached via cooling blocks to axially-, radially- or circumferentially-routed robust cooling tubes for trans-interface conductive heat removal. Coolant tubes may be in sliding grease contact with thermal supports onto which silicon detector substrates are glued (for example in the case of the ATLAS barrel pixel detector), may be embedded in heat conducting foam or may be rigidly attached to cooling blocks located under readout electronics at the perpihery of silicon (microstrip) sensors;
- **micro-channel** geometry (figs 6.2-6.5): with micro-channel cooling channels (of cross section 250 x 150 μm or less) etched into heat-sinks for pixelated detectors and their front-end readout electronics. This detector configuraton is clearly more adapted to small systems, but has a thermal figure of merit - expressed in terms of the temperature difference between the silicon substrate and the coolant for a given power density in $W.cm^{-2}$ – that can be superior (meaning a smaller temperature difference or offset giving a lower operating teperatre for a given cooling fluid temperature) by a factor of 10 or more compared to "tube and block" implementations [7.12].

Table 7.1: Cooling paramenters of most currently-operating CERN-based Si trackers.

Tracker	Tracker "DNA"	Primary coolant: (Liquid or evaporative)	Total *cooling power (kW)* & mass flow	On-detector tube *coolant temp (˚C)* & pressure (bar_{abs})	Typical Si Module temp (˚C)
ATLAS (SCT μ-strips & Pixels) [7.8], [7.9]	Tube & block	C_3F_8 (E)	*60* 1.2 kg/s	*SCT: -26 → -10 ˚C* 1.6 → 3 *Pixels: -24.5 ˚C* 1.7	SCT: - 7 → +7 ˚C (layer, disk dependent) Pixels: -14.5 ˚C
ATLAS (IBL) [7.11]	Tube & block	CO_2 (E)	*2* 30 g/s	*-20 ˚C* *20*	-13 ˚C
CMS (μ-strips) [7.7]	Tube & block	C_6F_{14} (L)	*34* (TIB, TID, TOB & TEC) 30 kg/s	*-15 ˚C* *6*	-10 → 0 ˚C (position depedent, single or double-sided modules etc.)
CMS Pixel upgrade [7.10]	Tube & block	CO_2 (E)	*15 (max)* 100 g/s	*-23 ˚C* *18*	-13 ˚C
LHCb VELO [7.12]	Micro-channel	CO_2 (E)	*1.6* 22.4 g/s	*-30 ˚C* *14*	-28 ˚C
TOTEM [7.13]	Tube & block	C_3F_8 (E)	*1.2* 40 g/s	*-26 ˚C* *1.6*	-15 ˚C
NA62 Gigatracker [7.5]	Micro-channel	C_6F_{14} (L)	*0.16* 12 g/s	*-14 → -12 ˚C* *3*	5 ˚C

Liquid C_6F_{14} cooling is successfully used in the NA62 Gigatracker: the first silicon microchannel vertex detector [7.5]. Liquid cooling can be attractive in such detectors since such liquid circulation systems typically operate at lower pressures than (particularly) CO_2-based evaporative cooling systems, although this latter technology has subsequently been mastered in the LHC VELO, as we have seen [7.12].

7.1.2 The substitution of perfluorohexane C_6F_{14} with $C_6F_{12}O$ fluoro-ketone

Thermophysical properties of C_6F_{14} and NOVEC 649 ($C_6F_{12}O$) fluoro-ketone [7.14], [7.15] are listed in Table 7.2. Evident similarities have made the substitution of C_6F_{14} with NOVEC 649 a potentially attractive option in future liquid-cooled systems, and motivated a detailed comparative study [7.16]

Table 7.2: Thermophysical Properties of NOVEC 649 **(**$C_6F_{12}O$) and C_6F_{14} (at 25ºC except where noted: after [7.15])

Fluid thermophysical property	NOVEC 649: $C_2F_5C(O)CF(CF_3)_2$ Perfluoro-2-methyl-3-pentanone ($C_6F_{12}O$ fluoro-ketone)	C_6F_{14} (Perfluorohexane, Saturated fluorocarbon)
Boiling temp @ 1 atm (˚C)	49	56
Critical Temp (˚C)	169	178
Critical Pressure (MPa)	1.87	1.89
Freezing temperatre (˚C)	< -100	< -100
Specific heat ($J.kg^{-1}K^{-1}$)	1103	1050
Density ($kg.m^{-3}$)	1610	1680
Kinematic viscosity (cSt)	0.42	0.4
Latent Heat ($J.kg^{-1}$)	88	88
Vapour Pressure @ 25 ˚C (kPa)	40.4	30.9
Vapour Pressure @ 100 ˚C (kPa)	441	350
Water solubility (ppm_w)	21	10

NOVEC 649 was as a result chosen as a liquid coolant for the silicon photomultipliers (SiPMs) of the new LHCb scintilating fibre (SciFi) tracker [7.4] , [7.5].

7.1.3 Speculative substitution of SFCs with fluoro-ketones for evaporative cooling at CERN

Evaporative fluorocarbon cooling was pioneered [7.8] for use in the ATLAS pixel and SCT microstrip tracker. Octafluoropropane (C_3F_8) primary coolant was initially circulated using a compressor system, recently replaced (from 2018) by a gravity-driven thermosiphon with a condenser located 90 metres above the ATLAS detector. The compressor system now serves as a back-up for the thermosiphon, which has the advantage of requiring no pumps or compressors in the C_3F_8 primary coolant loop.

It is possible that silicon tracker modules will need to be maintained at temperatures of -40 ˚C or below in future operation in the high luminosity phase of LHC - particularly after large accumulated radiation doses. Such effects will depend on detector fabrication technology and distance from to the LHC interaction point, but it can surmised from the silicon *module – coolant* temperature offsets shown in table 7.1 that trackers built in a ”block & tube” geometry (see fig. 3.4) will require lower coolant evaporation temperatures than microchannel devices. A plausible 10 ˚C safety margin for this *module – coolant* temperature offset would imply a corresponding in-tube evaporation temperature of -50 ˚C, which is uncomfortably close to the *triple point* limit of -56 ˚C for CO_2: CO_2 may not therefore be a long term solution.

Figure 7.2 (a)-(d) compares pressure-ethhalpy (*p-h*) diagrams for (a) octafluoropropane (C_3F_8), (b) CO_2, (c) hexafluoroethane (C_2F_6) and (d) xenon (Xe). Full circulator thermodynamic

cycles are not drawn, for the four fluids as these are highly system-dependent; for example with reversed rotation directions in the case of compressor *vs*. thermosiphon or CO_2 pumped accumulator [7.17] operation - and beyond the scope of this course. Nonetheless, some conclusions can be drawn from the bare *p-h* diagrams using simple indices.

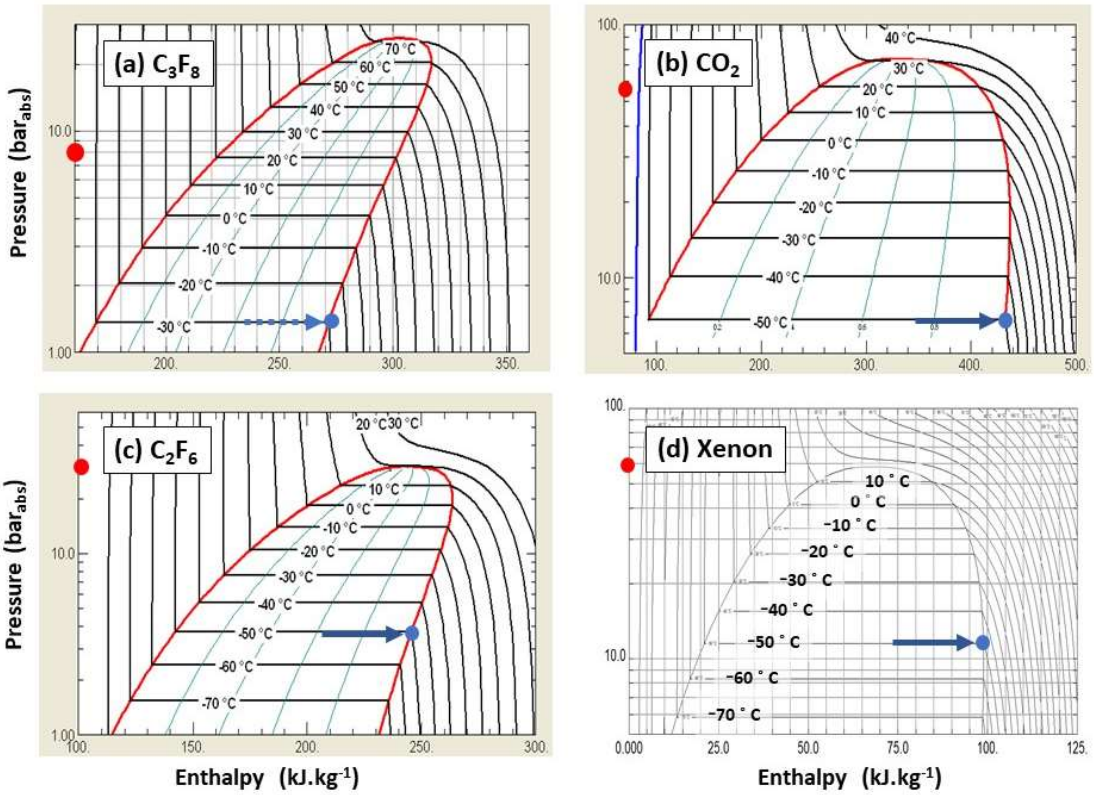

Fig. 7.2. Pressure-enthalpy (*p-h*) diagrams (after [7.18]) for (a) C_3F_8, (b) CO_2, (c) C_2F_6 & (d) Xe.
Red indices: saturation pressure at which cooldown from ambient temperature starts.
Blue indices: (a) C_3F_8 minimum practical in-tube evaporation temperature for a pressure of 1.5 bar; (b), (c) & (d) evaporation pressures in CO_2, C_2F_6 & Xe for in-tube evaporation temperaure of -50 ˚C.

On each *p-h* diagram red indices illustrate the fluid vapour pressure at an ambent temperature around 20 ˚C, from which detectors must be cooled to their operating temperatures. These pressures are respectively around 7.6, 57, 30 and 58 bar for C_3F_8, CO_2, C_2F_6 and Xe. It can be seen that CO_2 or xenon cooled systems will require the highest pressure tolerance by a large factor. This is further amplified since typical test and compliance pressures are typically more than a factor of two higher than the highest expected operation pressure [7.12].

In the case of C_3F_8 (fig. 7.2 (a)) - currently used in the ATLAS and TOTEM detectors – it is clear that the combination of an *in-tube* evaporation temperature of -50 ˚C at a minimal practical exhaust pressure of 1.5 bar_{abs} is thermodynamically impossible, clearly excluding this fluid for many future installations. However the dual constraints can be met with in CO_2, C_2F_6 and Xe (blue indices in fig. 7.2 (b), (c) & (d)) with respective exhaust pressures of 6.8, 4 and 12 bars. In the case of CO_2 however -50 ˚C is very close to the triple point temperature of -56 ˚C and probably represents the minimum safe system temperature. Of the four fluids C_2F_6 and xenon offer the best promise from a thermodynamic perspective, but C_2F_6 has a very high GWP and is likely to be prohibited in the near future.

Xenon is clearly a thermodynamic alternative to C_2F_6, as shown in fig 7.2 (d). It is a non-flammable radiation-resistant noble gas with a molecular weight (131) very close to that of C_2F_6 (138). There is considerable experience in its purificaton and thermodynamic circulation in dark matter detectors, where it is used in large (multi-tonne) quantities. This fluid is unlikely however - due to its scarcity and extremely high cost - to find use in secondary applications such as tracking detector cooling.

It is likely that all SFC fluids will be eliminated from use at CERN in the next decade. However following the $C_6F_{14}/C_6F_{12}O$ NOVEC649 analogy it is probable that a new zero-GWP NOVEC-like fluid with a spurred oxygen-bearing molecule of the form C_2F_4O (m.w.132) would have similar thermodynamic and thermophysical properties to its same-order similar molecular weight analogue - C_2F_6 (m.w.138). The industrialisation of new such fluids will probably depend, however, on future demand from the electronics industry for SFC replacements for SFCs, as has been the case for previously-developed zero-GWP NOVEC fluids.

7.1.4 So how is this relevant to evaporative cooling of processors at room temperature?

So how **IS** this relevant to evaporative cooling of processor chips at room temperature?

Well, as seen in fig 7.2, while C_3F_8 is not so good for use in large systems like those at CERN requiring evaporation at temperatures near -50 ˚C its thermodynamics is not so bad for use at room temperature (and not very different to the requirements of a domestic refrigerator). The evaporation pressure would be around 9 bar and the condensation (in a classic vapour compression cycle) would probably be around 20 bar, depending on the choice of condensation temperature.

However, since C_3F_8 is likely to be banned from many categories of use (and again using the $C_6F_{14}/C_6F_{12}O$ NOVEC649 analogy) it is probable that a new zero-GWP spurred oxygen-bearing molecule of the form C_3F_6O (m.w.166) would have similar thermodynamic properties to C_3F_8 (m.w.188). Only time will tell if the large-scale industrialisation of new such fluids will occur. How will the momentum to ban all fluorinated fluids be moderated by the massive economic driver of requirements from the electronics industry? We live in interesting times!

Last problem (7.1): see also separate sheet: – one for the sleuth:

While a new fluid C_3F_6O would have all the advantages of C_3F_8, but with zero GWP, the thermodynamics of C_3F_8 and presumably of C_3F_6O (which differs in molecular weight by 22 units) is not perfect for cooling a processor chip at room temperature. What fluid in the $C_nF_{2n}O$ spectrum might be better, and why?

Hint: the SFC progression of fig 7.2 may help in this.

References (by section)

Note: some references are repeated in different sections

Preamble

[P1] O. de Aguiar Francisco et al; 'Microchannel cooling for the LHCb VELO Upgrade I' Nucl. Instr. Meth A. 1039 (2022) 166874 https://www.sciencedirect.com/science/article/pii/S0168900222003394

Section (1)

[1.1] Proportional–integral–derivative controller - Wikipedia
[1.2] "Cooling a Superfast Computer": R. Danielson, N. Krejewski & J. Brost; Electronic Packaging and Production Vol 26(7) 1986 pp44-45
[1.3] https://www.datasheets.com/en/part-details/fc-77-3m-36336934

Section (2)

[2.1] E. Lemmon, M. Huber, & M. McLinden; REFPROP Standard reference database 23, version 9.0 (2010): U.S. National Institute of Standards & Technology.
[2.2] 3M Novec 649/1230 fluid ($C_6F_{12}O$) https://multimedia.3m.com/mws/media/569865O/3m-novec-engineered-fluid-649.pdf , https://multimedia.3m.com/mws/media/124688O/3m-novec-1230-fire-protection-fluid.pdf]
[2.3] https://multimedia.3m.com/mws/media/64892O/3m-fluorinert-electronic-liquid-fc72-en.pdf
[2.4] https://www.spacematdb.com/spacemat/manudatasheets/stycast2850.pdf

Section (3)

[3.1] E. Lemmon, M. Huber, & M. McLinden; REFPROP Standard reference database 23, version 9.0 (2010): U.S. National Institute of Standards & Technology
[3.2] D. Attree et al, 'The evaporative cooling system for the ATLAS inner detector' 2008 JINST 3 P07003 https://iopscience.iop.org/article/10.1088/1748-0221/3/07/P07003
[3.3] M. Battistin et al; 'The Thermosiphon Cooling System of the ATLAS Experiment at the CERN Large Hadron Collider' Int. J. Chemical Reactor Engineering 2015; 13(4): 511–521 https://www.degruyter.com/document/doi/10.1515/ijcre-2015-0022/html
[3.4] P. Dunn[1] & D. Reay[2]; [1]Reading University, UK, [2]Newcastle University, UK (emeritus) 'Heat Pipes' 4th Edition - 2016 Pergamon ISBN 13-978-0080419039
[3.5] https://en.wikipedia.org/wiki/Atmospheric_temperature

Section (4)

[4.1] It might seem a bit lame, but one could do worse than start in the usual place: https://en.wikipedia.org/wiki/Thermoelectric_cooling https://en.wikipedia.org/wiki/Thermoelectric_effect#Peltier_effect

Section (5)

[5.1] Vortex tubes: https://www.air-masters.eu/fr/49-tubes-vortex

Section (6)

[6.1] O. de Aguiar Francisco et al; 'Microchannel cooling for the LHCb VELO Upgrade I' Nucl. Instr. Meth A. 1039 (2022) 166874 https://www.sciencedirect.com/science/article/pii/S0168900222003394
[6.2] 3M Novec® range of fluorinated fluids; https://www.3m.com/3M/en_US/p/c/b/novec/?Ntt=novec
[6.3] D. Hellenschmdt et al; 'New insights on boiling carbon dioxide flow in mini- and micro-channels for optimal silicon detector cooling Nucl. Instr. Meth A. 958 April 2020, 162535 https://www.sciencedirect.com/science/article/pii/S0168900219310654
[6.4] https://www.youtube.com/watch?v=hsLXi9QTxUo

[6.5] https://www.youtube.com/watch?v=RmlQwLdfFZg

Section (7)

[7.1] 3M Fluorinert® range of fluorinated fluids;
https://www.3m.com/3M/en_US/p/?Ntt=fluorinert
[7.2] 3M Novec® range of fluorinated fluids
https://www.3m.com/3M/en_US/p/c/b/novec/?Ntt=novec
[7.3] L. Gruber et al; Nucl. Instr. & Meth. 958 (2020) 162025
https://www.sciencedirect.com/science/article/abs/pii/S016890021930422X?via%3Dihub
[7.4] C. Frei, S. Gambetta, B. Leverington; "Building the future of LHCb";
CERN Courier, September 2021 (2 September 2021)
https://cerncourier.com/a/building-the-future-of-lhcb
[7.5] G. Aglieri Rinella et al ; 'The NA62 GigaTracKer: a low mass high intensity beam 4D tracker with 65 ps time resolution on tracks', 2019 JINST 14 P07010
https://iopscience.iop.org/article/10.1088/1748-0221/14/07/P07010
[7.6] Understanding the stability and environmental characteristics of a sustainable Halon alternative
J. Owens, 3M Performance Materials 3M Center, St. Paul, MN 55144
https://www.nist.gov/system/files/documents/el/fire_research/R0301570.pdf
[7.7] P. Tropea; The CMS tracker fluorocarbon cooling system,
Engineering Forum: experiences from cooling systems for LHC detectors Oct 30 2008
https://indico.cern.ch/event/41288/contributions/1871985/attachments/842453/1171870/CMS_Fluorocarbon_Tropea.pdf
[7.8] D. Attree et al, 'The evaporative cooling system for the ATLAS inner detector'
2008 JINST 3 P07003 https://iopscience.iop.org/article/10.1088/1748-0221/3/07/P07003
[7.9] M. Battistin et al; 'The Thermosiphon Cooling System of the ATLAS Experiment at the CERN Large Hadron Collider' Int. J. Chemical Reactor Engineering 2015; 13(4): 511–521
https://www.degruyter.com/document/doi/10.1515/ijcre-2015-0022/html
[7.10] W. Adam et al ; 'The CMS Phase-1 pixel detector upgrade' 2021 JINST16 P02027
https://iopscience.iop.org/article/10.1088/1748-0221/16/02/P02027
CMS Technical Design Report for the Pixel Detector Upgrade CMS-TDR-011, CERN-LHCC-2012-016
07/09/2012 https://cds.cern.ch/record/1481838/files/CMS-TDR-011.pdf
[7.11] ATLAS Insertable B-Layer Technical Design Report; CERN-LHCC-2010-013 ATLAS TDR 19
15/09/2010 https://cds.cern.ch/record/1291633/files/ATLAS-TDR-019.pdf
[7.12] O. de Aguiar Francisco et al; 'Microchannel cooling for the LHCb VELO Upgrade I'
Nucl. Instr. Meth A. 1039 (2022) 166874
https://www.sciencedirect.com/science/article/pii/S0168900222003394
[7.13] G. Anelli et al ; 'The TOTEM Experiment at the CERN Large Hadron Collider'
2008 JINST 3 S08007 https://iopscience.iop.org/article/10.1088/1748-0221/3/08/S08007
[7.14] 3M Novec 649/1230 fluid (C6F12O);
https://multimedia.3m.com/mws/media/569865O/3m-novec-engineered-fluid-649.pdf,
https://multimedia.3m.com/mws/media/124688O/3m-novec-1230-fire-protection-fluid.pdf]
[7.15] "Fluoroketone $C_2F_5C(O)CF(CF_3)_2$ as a Heat Transfer Fluid for Passive and Pumped 2-Phase Applications"; P. Tuma, 3M Co., 3M Center, 236-2B-01St. Paul, MN 55144, USA,
Proc. IEEE 24th IEEE Semiconductor Thermal Measurement and Management Symposium, San Jose CA, March 16-20 2008 DOI: 10.1109/STHERM.2008.4509386
also accessible via:
https://twiki.cern.ch/twiki/pub/LHCb/SciFiDemoCooling/F.Tuma_c6K_as.....pdf
[7.16] CERN report EN-CV 22/12/2017, EDMS 1751219 2017-334 rev 1.0: Technical Note NOVEC Fluids Qualification Report: Report on the study executed for the qualification of the NOVEC Fluid for Detector Cooling applications.
[7.17] B. Verlaat; CO_2 cooling experiences in the LHCb Velo Thermal Control System
Engineering Forum: experiences from cooling systems for LHC detectors Oct 30 2008
[7.18] E. Lemmon, M. Huber, & M. McLinden; REFPROP Standard reference database 23, version 9.0 (2010): U.S. National Institute of Standards & Technology